F L

Issued also as ARL 63-74

AN EXPERIMENTAL INVESTIGATION OF THE SEPARATION OF A HYPERSONIC BOUNDARY LAYER ON A FLAT PLATE

Part I: Pressure distribution and optical studies at M = 11.7

W. J. Graham and I. E. Vas

Princeton University

February 1963 Report 631

631

Sups
AD-406702

PRINCETON UNIVERSITY

DEPARTMENT OF AERONAUTICAL ENGINEERING

ARL-63-74

AN EXPERIMENTAL INVESTIGATION OF THE SEPARATION OF A HYPERSONIC BOUNDARY LAYER ON A FLAT PLATE

Part I: Pressure distribution and optical studies at M = 11.7

W. J. Graham and I. E. Vas

Princeton University

February 1963 Report 631

Contract AF 33(616)-7629
Project No. 7064
Task No. 70169

Aeronautical Research Laboratory
Office of Aerospace Research
United States Air Force
Wright-Patterson Air Force Base, Ohio

FOREWARD

The present study is part of a program of theoretical and experimental research on hypersonic flow being conducted by the Gas Dynamics Laboratory of the Department of Aeronautical Engineering at the James Forrestal Research Center, Princeton University. This study is sponsored by the Aeronautical Research Laboratory, Wright Air Development Division, under Contract AF 33(616)-7629, "Research on Boundary Layer Characteristics in the Presence of Pressure Gradients at Hypersonic Speeds", with Capt. W. W. Wells and Col. A. Boreske as consecutive project officers.

The advice received from Prof. S. M. Bogdonoff was of great assistance during the entire study.

ABSTRACT

A study was carried out in the Princeton University 3 inch helium hypersonic wind tunnel at a Mach number of 11.7 to examine the flow over a flat plate with disturbances located at a distance from the leading edge. The leading edge Reynolds number was varied from 190 to 20,900. The disturbances, varying in shape from a 10^{o} to a 30^{o} wedge, a 90^{o} step and one with a hemicylindrical shape, were investigated over the leading edge Reynolds number range. Schlieren photographs and detailed surface pressure distributions were obtained to determine the location of the separation point and the pressure ratio across the separation region.

TABLE OF CONTENTS

NOMENCLATURE

d	Distance from separation pressure rise to corner at intersection of flat plate and wedge or step
h	Afterbody height
M	Mach number
p	Measured pressure on the model surface
$p_{f.p.}$	Measured pressure on the flat plate without any disturbance
p_o	Stagnation pressure
p_l'	Free stream static pressure on tunnel axis (varies with distance along axis)
$\Delta p = p - p_l'$	
$Re_{l,t}$	Reynolds number based on leading edge thickness and free stream conditions
t	Leading edge thickness
x	Distance from leading edge
θ_d	Angle separated boundary layer makes with flat plate surface
θ_w	Wedge angle
ξ	Streamwise coordinate, measured from the junction of the flat plate and afterbody

INTRODUCTION

The study of boundary layer separation has been the subject of many studies, both theoretical and experimental, during the past decade. A considerable amount of work has been concerned with this phenomenon at supersonic speeds (Refs. 1 to 6); but results at hypersonic speeds, where the problem is complicated by entropy and pressure gradients, is quite sparse. The present work is part of a long range program to study the hypersonic boundary layer, its separation characteristics, and to determine the parameters involved. The work reported herein was concerned with the simplest conditions which could be generated, a two-dimensional flow over a flat plate with variable thickness leading edge. The disturbances, located at a distance from the leading edge, were also two-dimensional and varied from a wedge to a 90° step. The optical and surface pressure distribution studies were conducted at a free stream Mach number of 11.7 using helium as the test fluid.

The work of Ref. 7, which detailed the flow over the basic flat plate with variable thickness leading edges, was used as the base results, and the influence of the disturbances on these flows was the subject of the present investigation.

TEST FACILITIES AND MODELS

The test program was carried out in the Princeton University helium hypersonic wind tunnel (Ref. 8, Fig. 1). A contoured nozzle was used which gave a Mach number of 11.7 ± 0.25 over an axial length of about

7 inches. The tests were carried out at a stagnation pressure of 1000 psia with a stagnation temperature of about 75°F. For these conditions, the free stream Reynolds number was 10^6 per inch. Running times of several minutes were available to insure thermal equilibrium.

The model consisted of a flat plate with various-shaped after bodies mounted on it, Fig. 2. The basic flat plate was made from ¼ inch thick flat ground stock, 2 inches wide and about 4 inches long. The leading edge was formed by grinding a 10° wedge off the bottom surface and the leading edge thickness was varied by cutting off material normal to the test surface. Afterbodies were attached to the flat plate 2 inches from the leading edge and consisted of wedges with angles of 0°, 10°, 20°, 30° and 90° (a step). In addition, a hemicylindrical step was also used (Fig. 2b). All these afterbodies had a height of 0.2 inches and an additional afterbody of the 10° wedge was made with a height of 0.4 inches. The total length of the flat plate formed with the "0°" wedge was 4.27 inches. The joint between the plate and the afterbodies was sealed with clear lacquer to prevent leakage. When pressure distribution and separation results were being obtained, the models were equipped with side plates which completely enclosed the separated region (see Fig. 2a). For optical studies, these side plates were removed. Their removal noticeably affected the measured pressure distribution so that the optical studies can only be considered as quantitative.

Static pressure orifices were located along the center line of the model. These orifices were connected to manometers using silicone oil or mercury by means of copper tubing. The reference pressure for these manometers was kept at about 20 microns.

Schlieren photographs were taken of the flow about the body using a two-mirror, on-axis spark system with a spark duration of about 1 microsecond. A horizontal knife edge was generally used.

RESULTS AND DISCUSSION

Several investigations have been conducted on the phenomenon of separation of a laminar boundary layer ahead of a step in a supersonic stream. A uniform external stream existed and separation occurred in a boundary layer whose characteristics were well known. For the hypersonic case, the problem is complicated by the fact that the boundary layer-leading edge shock interaction induces a flow field over the entire plate. As the leading edge thickness is increased, the conditions over the plate vary: for very thin leading edges the effects are primarily viscous, for very thick leading edges the effects are due to the nose itself and are primarily inviscid. At a given station on the plate, a change in the leading edge dimension results in changes in the thickness and profile of the boundary layer, the pressure gradient and level along the wall, and the Mach number and normal entropy gradients at the outer edge of the boundary layer.

At these hypersonic speeds, little detailed experimental information is available on the two-dimensional separation phenomenon. Some data are available for conditions ahead of a forward facing step at a Mach number of 6.5 in air (Ref. 9) and some previous results from the Princeton University Gas Dynamics Laboratory show the strong effects of trailing edge flaps for Mach numbers up to 13 in helium. The present work is an attempt to repeat the well known systematic variations of the

supersonic studies under hypersonic conditions with its attendant leading edge complications.

In a previous paper (Ref. 7), the details of the flow over a flat plate at a Mach number of 11.7 with leading edge thicknesses from 0.2×10^{-3} to 21.8×10^{-3} inches were obtained. The present paper considers the same Mach number and range of leading edge thicknesses so that the results of Ref. 7 are used as the "no disturbance" case. Some typical schlieren photographs of the flow over the flat plate are shown in Fig. 3 and the measured pressure distributions in Fig. 4. For each leading edge condition, the flow over the flat plate and the disturbance were studied for the various disturbances.

OPTICAL STUDIES

Schlieren photographs were taken for each test configuration (without side plates). Some typical photographs are shown in Figures 5 to 7.

In Figure 5, the effect of the disturbance on the flat plate with ed leading edge thickness is seen. The three shocks, at the lead- dge, separation and reattachment are well defined. The turning of the flow as indicated by the edge of the boundary layer is also quite clearly seen. The separation point (as roughly defined by the initial turning of the boundary layer) is seen to move forward as the wedge angle is increased.

The effect of the leading edge thickness on the flow over a flat plate with a 10° wedge is shown in Fig. 6a, c, d. As the leading edge thickness is increased, the separation point moves closer to the

junction of the plate with the wedge. The shocks caused by the turning of the flow due to separation and reattachment are quite distinct for the thin leading edge, but merge to form a single shock for $t = 21.8 \times 10^{-3}$ inches.

For the same leading edge thickness, the 10° wedge was changed from 0.2 inches to 0.4 inches to evaluate the effect of the downstream boundary of the wedge, Fig. 6b.

The other extreme for a disturbance on the flat plate was a 90° step, or a forward facing step (Fig. 7). For the thin leading edge, the separation starts close to the leading edge. In fact, for $t = 1.7 \times 10^{-3}$ inches, it was impossible to establish the flow (the tunnel would not start). As the leading edge thickness increases, the separation occurs further back on the plate. In all cases, the reattachment seemed to be at the top corner of the step.

The angle which the separated boundary layer makes with the flat plate was measured for all conditions. The separation angle, θ_d, is plotted against the forward propagation distance, d (Fig. 8). There is considerable scattering of the data for leading edge thicknesses of 5.1×10^{-3} inches and less. The overall separation angle variation is from 3.5° to 8° for wedge angles from 10° to 90°. For leading edge thicknesses equal to 5.1×10^{-3} inches and less, the separation angle seems to be independent of the wedge angle for the same forward propagation distance. However, as the leading edge thickness increases, the separation angle increases, and at a value of $t = 21.8 \times 10^{-3}$ inches, θ_d is approximately 50% more than the value for the thin leading edges.

It should be pointed out that the values of θ_d were obtained from pictures taken of the model without side plates. Hence the data should only be considered qualitative. However, as the initial pressure rise does not seem to be strongly affected by absence of the end plates (see next section) the measured values of θ_d are a very good approximation to those that would have been obtained were end plates used.

PRESSURE DISTRIBUTION STUDIES

The pressures measured on the flat plate and afterbody are presented as the ratio of the measured pressure, p, to the local tunnel pressure p_1', as a function of the distance ξ measured from the junction of the flat plate surface with the step. In order to keep the flow over the surface free from three-dimensional effects, all pressure distribution studies were carried out with end plates sealed to the sides of the model. The effects of the flow over the plate with a 10^o wedge with and without side plates is shown in Fig. 9 and larger effects were found for stronger disturbances.

The detailed pressure distributions are summarized in Figs. 10 to 12. In Fig. 10, the pressure distributions with a 10^o wedge of two heights for plate leading edge thicknesses of 0.2, 0.8 and 5.1×10^{-3} inches are presented. Since this interaction was the weakest studied, considerable attention was paid to the effect of downstream disturbances on the separation phenomenon and so two wedge heights or lengths were examined. As can be seen, although an effect of changing the wedge height was found, its effects were relatively small in the region of interest. The absence of any effect on the pressure distribution caused by increasing the 10^o wedge height from 0.2 to 0.4 inches is considered

important in extending the above results to the general case of separation ahead of a wedge whose height is greater than the boundary layer thickness.

The calculated inviscid wedge pressure based on free stream conditions is shown on all the figures although a better prediction is obtained if the Mach number and static pressure at the separation point is used. For purposes of clarity, the beginning of the pressure rise (deviation of the measured pressure from that found on the basic flat plate) is termed the "separation point". This is not actually the "point" at which separation occurs, but separation does appear close to this point, as determined from oil trace studies. Between the separation point and the junction of the wedge with the flat plate, the pressure rises slowly with an inflection point in the curve occurring close to the beginning of the wedge. The pressure gradient on the wedge is considerably greater than over the plate and exhibits no strong variation around the reattachment point. The pressure distributions for the various disturbances for each of the leading edge thicknesses are shown in Fig. 11. Choking of the tunnel occurred for all models at $t = 0.2 \times 10^{-3}$ inches except for the 10° wedges.

The pressure distributions in the separation regions in all cases resemble those associated with pure laminar separation at supersonic Mach numbers (Refs. 3 and 5). The pressure rises as the boundary layer separates from the surface and then remains almost constant along the separation region until the upstream edge of the disturbance is approached. A small dip in the pressure curves just before the disturbance is typical for strong disturbances and is associated with the

generation of a small secondary vortex in the corner. On a plate of given leading edge thickness, the forward propagation of separation is strongly affected by the disturbance used (Figs. 10 and 11). For example, in the case of $t = 12.7 \times 10^{-3}$ inches (Fig. 11d), the square step causes the separation pressure rise 1.5 inches (or 7.5 step lengths) ahead of the corner. Rounding the step or reducing the wedge angle results in the beginning of separation moving downstream until, in the case of a 10^{o} wedge, it lies only 0.4 inches ahead of the corner. The beginning of separation moves downstream into a region of increased Mach number and increased boundary layer thickness. The gradients in the reattachment region go up sharply as the disturbance gets stronger (varying from the 10^{o} wedge towards the step).

For a given wedge configuration the leading edge thickness strongly affects the forward propagation of separation, as shown in Fig. 12. For example, in the case of a 30^{o} wedge (Fig. 12b) the pressure rise occurs 1.5 inches ahead of the corner for $t = 0.8 \times 10^{-3}$ inches. The Mach number at the edge of the boundary layer at the separation point is about 8 (Ref. 7). As the leading edge thickness is increased to 21.8×10^{-3} inches, the separation moves back to a point 0.9 inches ahead of the corner. At this position, the Mach number at the boundary layer edge is about 3.5. In the case of a 10^{o} wedge with $t = 21.8 \times 10^{-3}$ inches the separation point has moved back until the pressure rise across the interaction has no inflection point (Fig. 12a) and the separation region has almost disappeared (Fig. 6d).

For all disturbances, the general trends were the same: blunting the leading edge decreased the extent of the separated region. The

separation point moves back towards the disturbance and occurs in a region of lower Mach number. Blunting increases the pressure level over the plate and also results in much stronger entropy variations outside the boundary layer.

The forward propagation of separation or the pressure rise is summarized in Fig. 13 with a plot of the forward propagation distance, d, versus $\log t$. The lower limitations on leading edge thickness for the 20° and 30° wedges, and the rounded and square step models were caused by tunnel choking. The 10° wedge results show a well established maximum forward propagation for thin leading edges and what looks like a minimum for thick leading edges. The curves corresponding to the other wedges and steps appear to have the same form, and presumably would approach similar limits if the tunnel could be operated for the thin leading edges and the tests were extended to even blunter leading edges.

PRESSURE RATIO ACROSS SEPARATION

The work done on separation of boundary layers in supersonic flow (Refs. 3 and 5) has shown that the pressure ratio across separation ("plateau" pressure ratio, the ratio of the maximum pressure reached in the forward part of the separated region divided by the pressure on the undisturbed plate) is an important parameter in describing the flow. In the supersonic studies, the undisturbed flow resulted in a constant pressure along the plate. In the present series of tests, separation is superimposed on a favorable pressure gradient whose strength depends on the position of separation and on the leading edge thickness. Under these conditions, two pressure ratios can be calculated: (1) non-dimensionalizing by the pressure at the separation point, and (2) non-dimensionalizing by

the pressure on the undisturbed flat plate at corresponding streamwise stations. Since, for some cases, there are strong variations in pressure along the plate without the disturbance, the latter method was chosen. The pressure ratio thus calculated is a measure of the local disturbance caused by the wedge or step and such results are presented in Figs. 14 and 15, where $P/P_{F,P}$ is plotted versus x. Figure 14a shows the effect of varying wedge angle on the flat plate with a leading edge thickness 0.8×10^{-3} inches. Similar plots for $t = 5.1$ and 21.8×10^{-3} inches are shown in Figs. 14b and 14c. The effect of varying leading edge thickness for a given wedge or step configuration is shown in Fig. 15 for the 10° and 30° wedges and square step. In nearly all of the cases studied, the pressure curves approach a plateau value of pressure ratio in the separated region. This value is referred to as the "pressure ratio across separation". A plateau pressure is not reached for the 10° wedge except for the thinnest leading edge case and for several of the other configurations although the gradients become quite small.

It is seen from Fig. 14 that, as the point of separation moves forward on the given flat plate (into a region of lower M and reduced boundary layer thickness), the pressure ratio across separation is increased. For example, on the flat plate with $t = 5.1\times10^{-3}$ inches (Fig. 14b), the pressure ratio increases from about 2.0 to 2.75 as the wedge angle is increased from 20° to 90°. This corresponds to the measured boundary layer separation angle (θ_d) increasing from 5° to 6° (Fig. 9).

Figure 15 shows that, as the leading edge thickness is increased and the Mach number at the boundary layer edge is decreased, the separation point moves back and the separation pressure ratio is decreased for a given wedge or step. For example, in the case of the square step (Fig. 15c), the

pressure is 2.8 for $t = 5.1 \times 10^{-3}$ inches and is reduced to 2.35 at $t = 21.8 \times 10^{-3}$ inches.

In the case of the flat plate with a leading edge thickness of 21.8×10^{-3} inches, he Mach number at the edge of the boundary layer is known to ve about 3 to 4 in the region where separation is occurring (Ref. 7). Thus the pressure ratio across separation can be compared with that presented by Gadd in Ref. 5 for separation at similar Mach numbers in air. Their results are shown in Fig. 14c for both laminar and turbulent separation. The turbulent pressure ratio is shown for the flow ahead of a square step. The present tests show the pressure ratio across separation to be higher than the laminar value (about 1.25) but less than the turbulent value (between 2.9 and 3.7): the pressure ratio ahead of the square step for $t = 21.8 \times 10^{-3}$ inches is 2.35. A study is presently being conducted to determine the detailed heat transfer on a similar flat plate at a Mach number of 12 in helium. The preliminary results show a continuously decreasing heat transfer over the entire model indicating that a laminar boundary layer exists on the surface. No detailed results have been obtained on the boundary layer once it has separated. From the schlieren photographs of the separated flow configurations, it is <u>not</u> possible to state with certainty that the boundary layer is laminar through reattachment. As the pressure ratio across separation seemed to be high for the laminar case and low for the turbulent case, the boundary layer could possibly be transitional through the separation region. Further work on the separated boundary layer will be necessary to clarify this point. This uncertainty in the boundary layer characteristics after separation (see for example, Fig. 7, a and c) is the major point which must qualify the conclusions of the present work.

CONCLUDING REMARKS

The separation phenomenon on a flat plate in hypersonic flow is strongly dependent upon the leading edge conditions. The entire pressure distribution on the model can be changed by modifying the leading edge thickness. Hence, separation can occur on the plate either at high Mach numbers (occurring if the leading edge thickness is small) or low Mach numbers (if the leading edge thickness is large). It is also important to point out that the separation phenomenon takes place in a favorable pressure gradient.

In the present study, the leading edge thickness was varied so that the Mach number at the beginning of separation varied from 10 to 3. The length of the flat plate was kept constant and under most conditions, the height of the disturbance was held at 0.2 inches. However, for the single case of a 10° wedge this height was doubled and no effect of this change was noted in the separation-reattachment region. For a fixed leading edge thickness and wedge height, the forward propagation of the separation point increased as the wedge angle increased.

The pressure ratio across separation (based upon the undisturbed flat plate distribution) increased as the separation point moved towards the leading edge. This was accomplished either by increasing the wedge angle for fixed leading edge thickness or decreasing the leading edge thickness for fixed wedge angle. The measured pressure ratios across separation were higher than those measured in air for the laminar case (at the same local Mach number at the separation point) but was less than the corresponding turbulent values.

More detailed studies of the separated boundary layer are required to determine whether transition might be affecting the presented results although the boundary layer on the flat plate was laminar.

BIBLIOGRAPHY

1. Crocco, L. and Lees, L.: A Mixing Theory for the Interaction Between Dissipative Flows and Nearly-Isentropic Streams. Princeton University Aeronautical Engineering Department Report 187, January 1952.

2. Chapman, Dean R.: A Theoretical Analysis of Heat Transfer in Regions of Separated Flow. NACA TN 3792, October 1956.

3. Chapman, D. R.; Kuehn, D. M. and Larson, H. K.: Investigation of Separated Flows in Supersonic and Subsonic Streams With Emphasis on the Effect of Transition. NACA TN 3869, March 1957.

4. Larson, Howard K.: Heat Transfer in Separated Flows. IAS Report No. 59-37, January 1959.

5. Gadd, G. E.; Holder, D. W. and Regan, J. D.: An Experimental Investigation of the Interaction Between Shock Waves and Boundary Layers. Proc. Roy. Soc., A, Vol. 226, 227-253, 1954.

6. Bogdonoff, S. M.: Some Experimental Studies of the Separation of Supersonic Turbulent Boundary Layers. Princeton University Aeronautical Engineering Department Report 336, June 1955.

7. Graham, W. J. and Vas, I. E.: The Effect of Leading Edge Conditions on the Detailed Flow Over a Flat Plate at M = 11.7. Princeton University Aeronautical Engineering Department Report 565, September 1961; also ARL 138.

8. Bogdonoff, S. M. and Hammitt, A. G.: The Princeton Helium Hypersonic Tunnel and Preliminary Results Above M = 11. Princeton University Aeronautical Engineering Department Report 260, June 1954; also WADC TN 54-124, July 1954.

9. Sterrett, J. R. and Emery, J. C.: Extension of Boundary-layer-separation Criteria to a Mach Number of 6.5 by Utilizing Flat Plates with Forward-facing Steps. NASA TN D-618, December 1960.

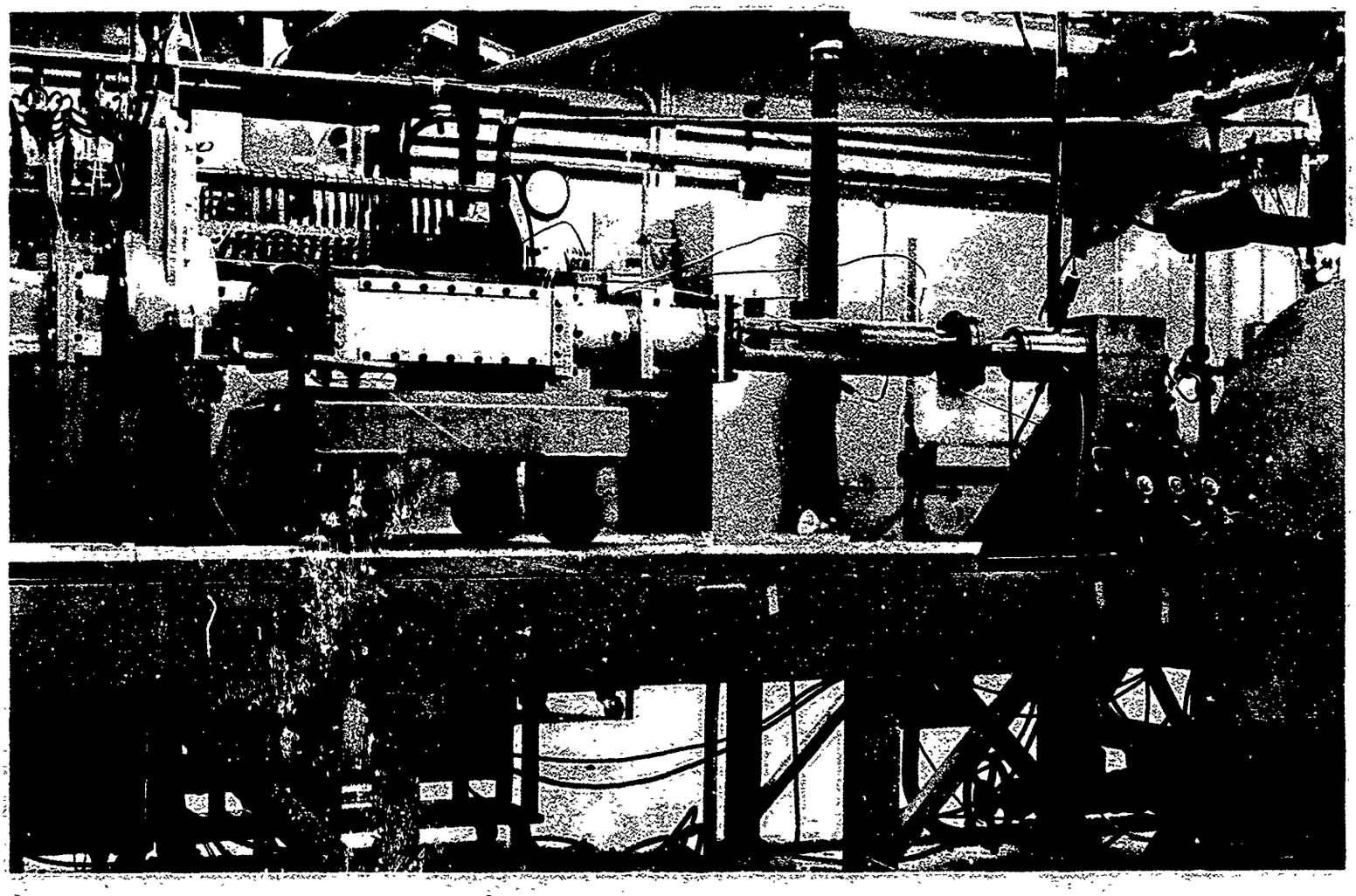

Figure 1. The Princeton University Helium Hypersonic Wind Tunnel.

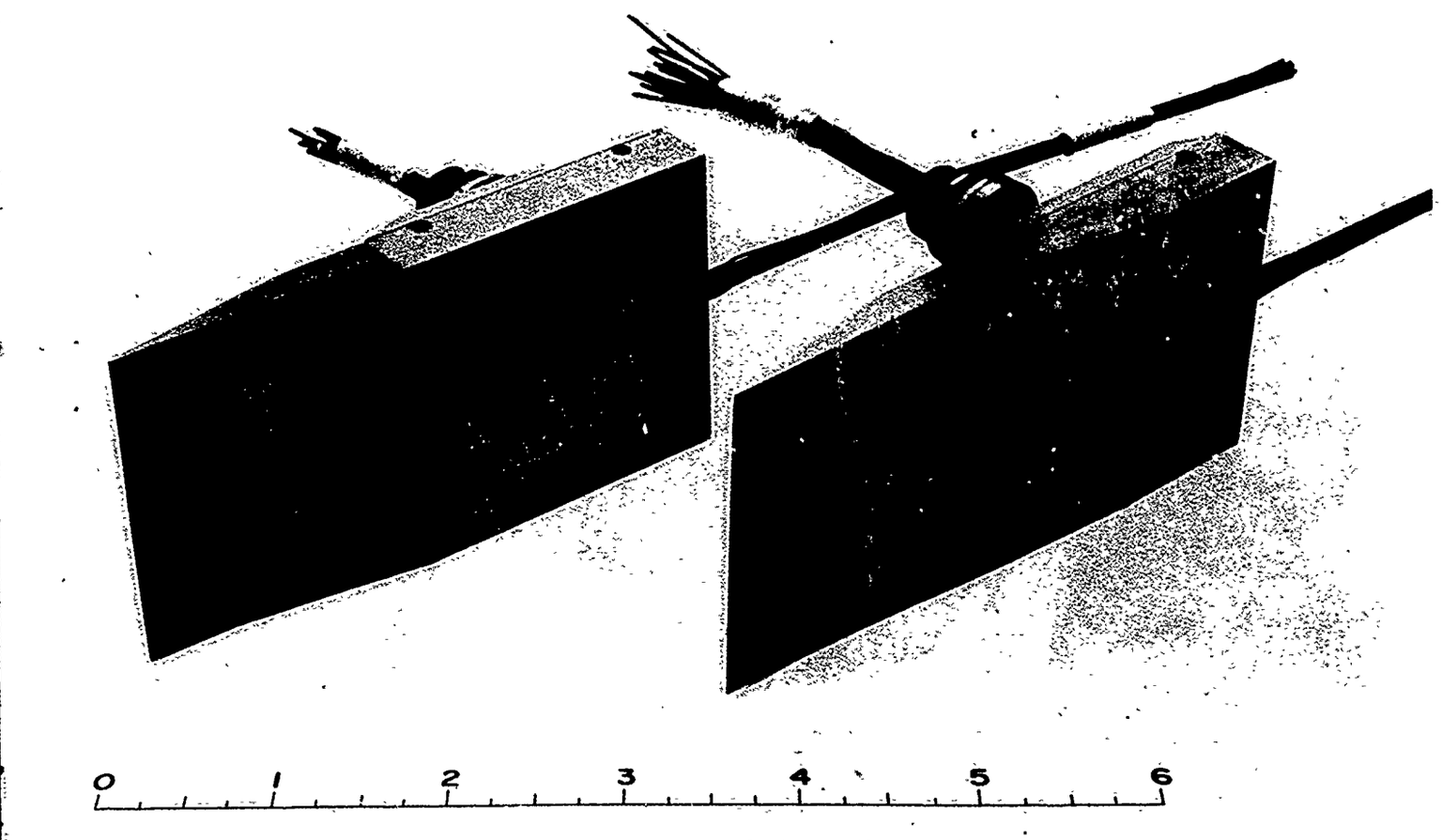

Figure 2a. Photograph of the flat plate with afterbody attached and end plates on one side

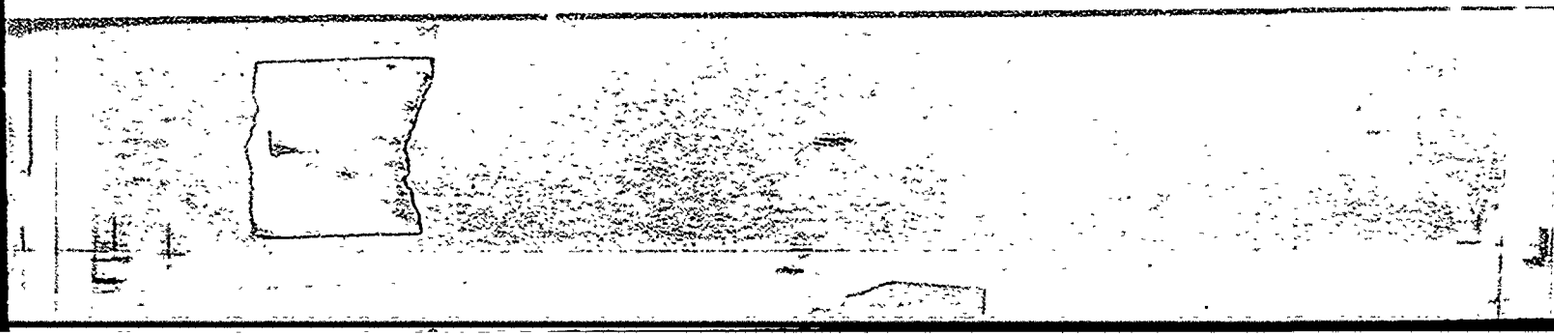

a) $t = 0.20 \times 10^{-3}$ inches

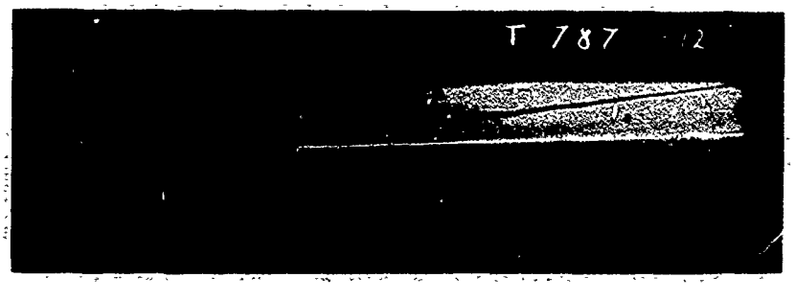

b) $t = 0.80 \times 10^{-3}$ inches

c) $t = 5.10 \times 10^{-3}$ inches

d) $t = 12.7 \times 10^{-3}$ inches

Figure 3. Schlieren photographs of the flow over a flat plate at M=11.7 for various leading edge thicknesses

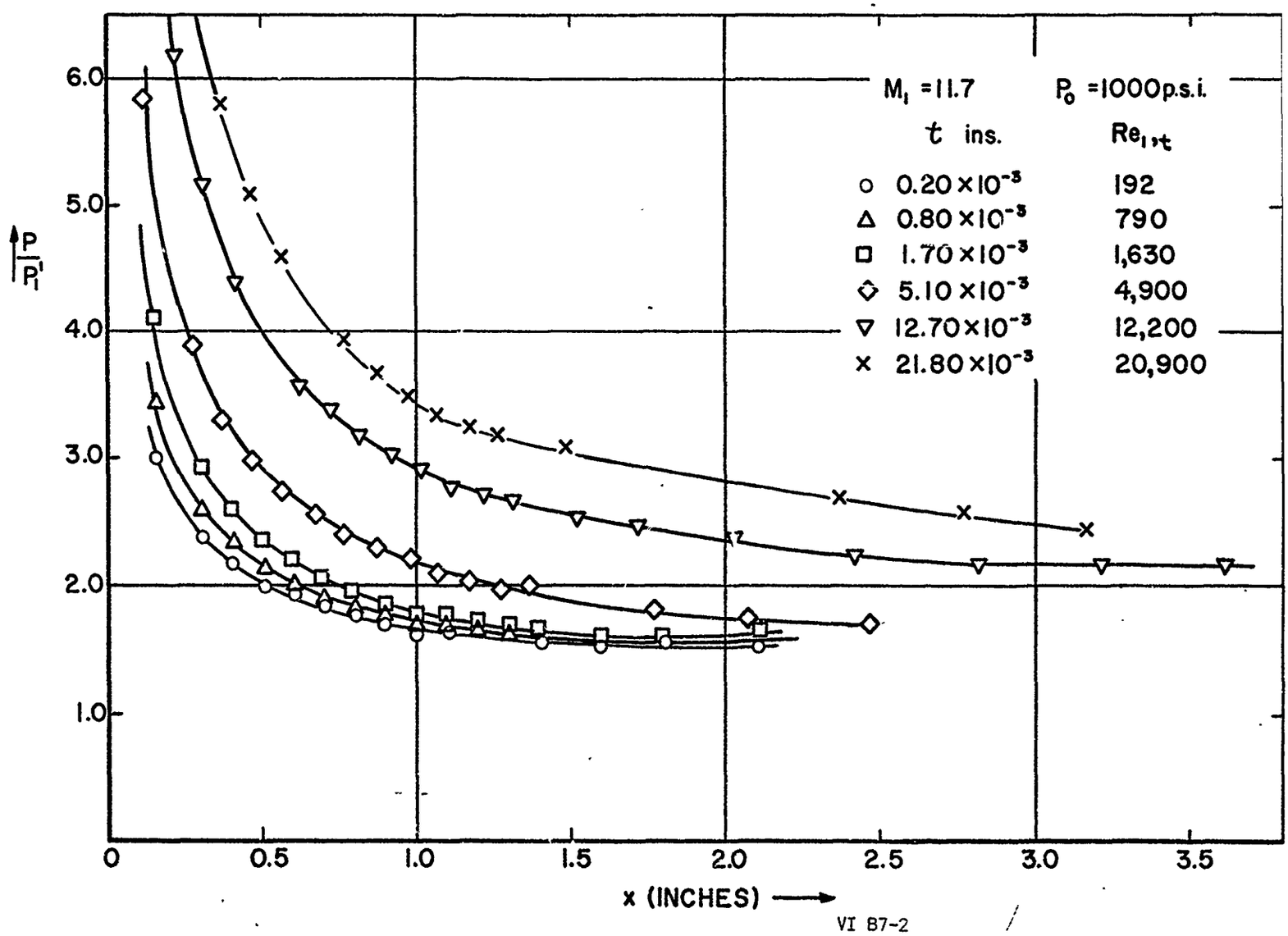

VI B7-2

Figure 4. The pressure distribution on a flat plate at M ~ 11.7 for varying leading edge thicknesses

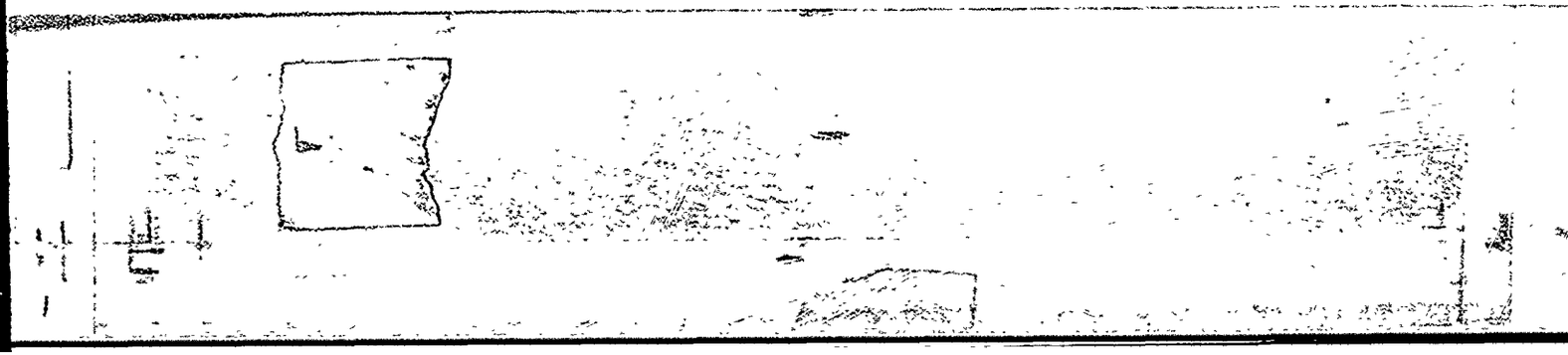

a) 10° wedge, h=0.2 inches

b) 20° wedge, h=0.2 inches

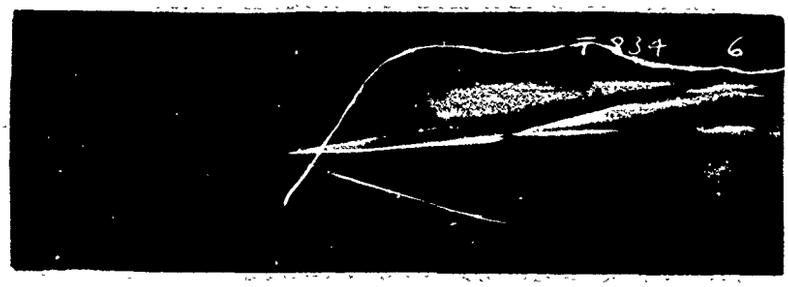

c) 30° wedge, h=0.2 inches

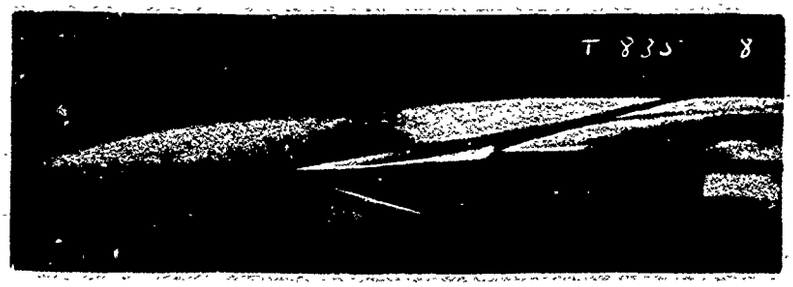

d) hemicylindrical step, h=0.2 inches

Figure 5. Schlieren photographs of the separated flow on a flat plate at $M = 11.7$ for various afterbodies, $t = 1.7 \times 10^{-3}$ inches

a) $t = 0.20 \times 10^{-3}$ inches, $h = 0.2$ inches

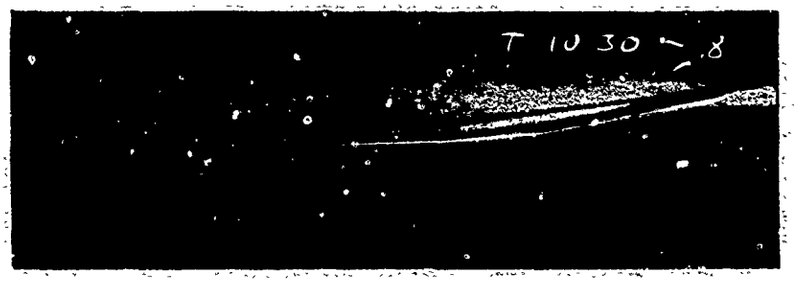

b) $t = 0.20 \times 10^{-3}$ inches, $h = 0.4$ inches

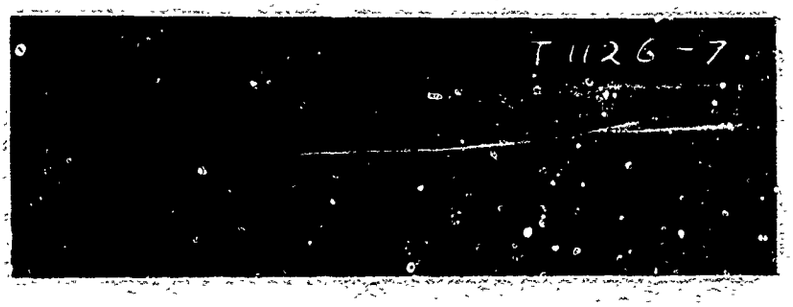

c) $t = 1.7 \times 10^{-3}$ inches, $h = 0.2$ inches

d) $t = 21.6 \times 10^{-3}$ inches, $h = 0.2$ inches

Figure 6. Schlieren photographs of the flow over a flat plate and 10° wedge at $M = 11.7$ for various leading edge thicknesses and wedge height

a) $t = 0.20 \times 10^{-3}$ inches, h = .2 inches

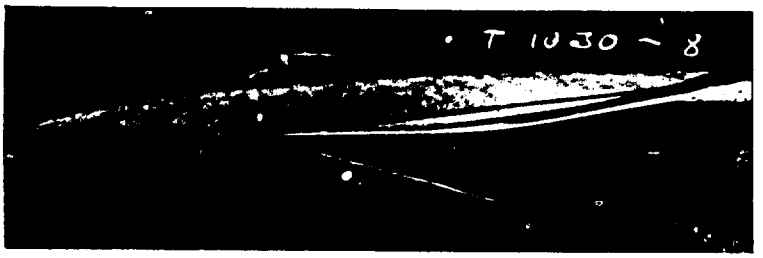

b) $t = 0.20 \times 10^{-3}$ inches, h = 0.4 inches

c) $t = 1.7 \times 10^{-3}$ inches, h = 0.2 inches

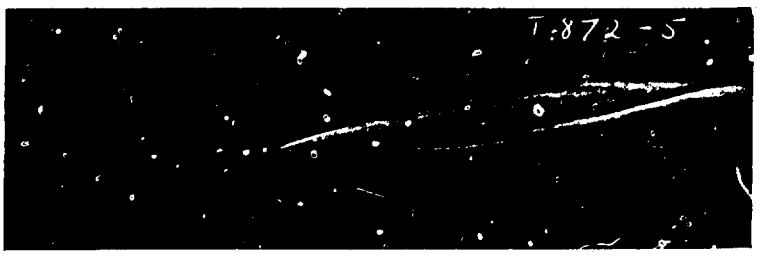

d) $t = 2.6 \times 10^{-3}$ inches, h = 0.2 inches

Figure 6. Schlieren photographs of the flow over a flat plate and 10° wedge at M = 11.7 for various leading edge thicknesses and wedge height

a) $t = 5.1 \times 10^{-3}$ inches, $h = 0.2$ inches

b) $t = 12.7 \times 10^{-3}$ inches, $h = 0.2$ inches

c) $t = 21.8 \times 10^{-3}$ inches, $h = 0.2$ inches

Figure 7. Schlieren photographs of the separated flow on a flat plate ahead of a 90° step at M = 11.7 for various leading edge thicknesses

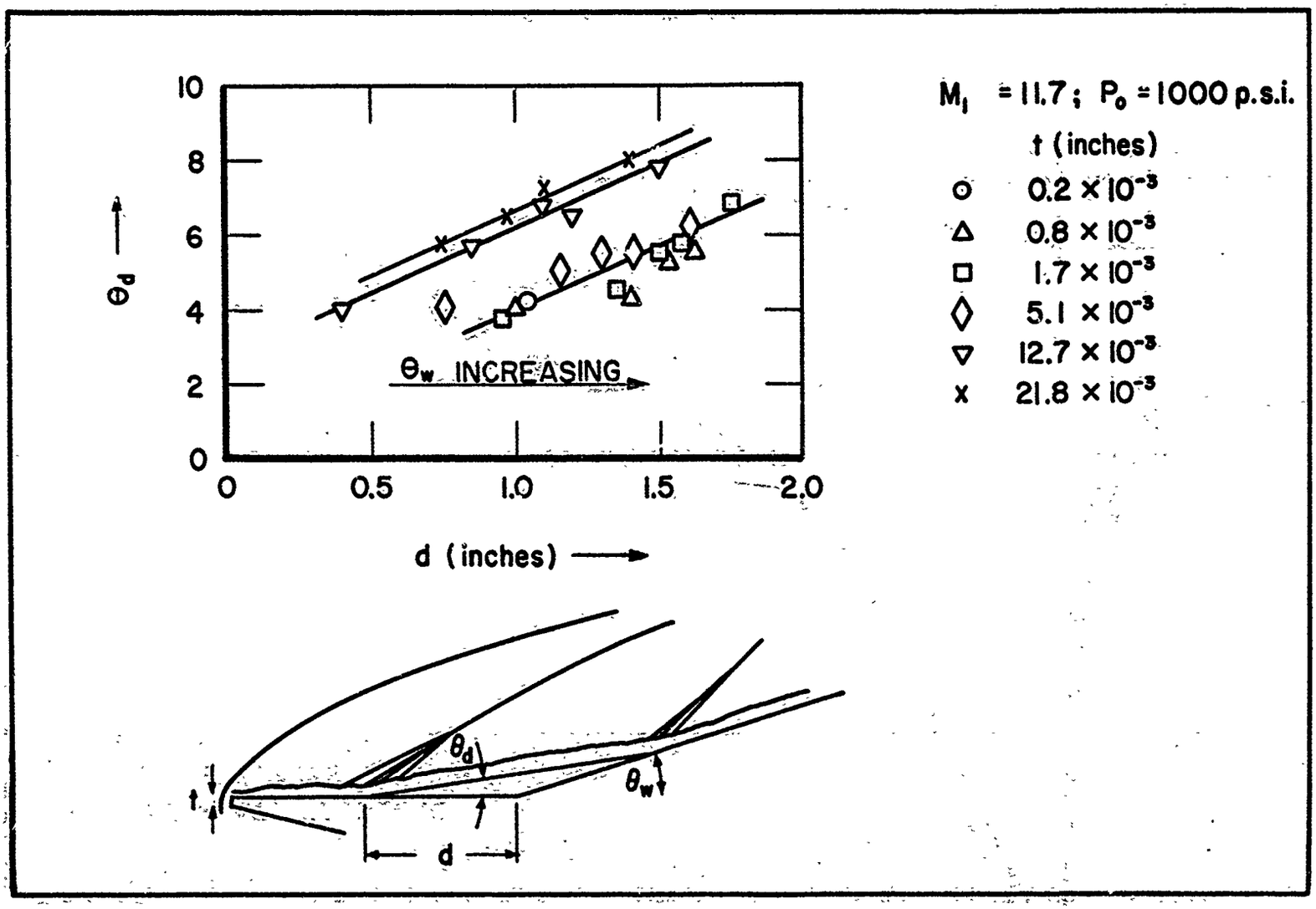

XII B2-2

Figure 8. Variation of boundary layer separation angle with forward propagation of separation.

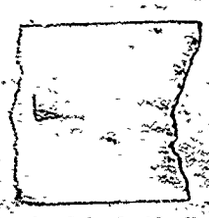

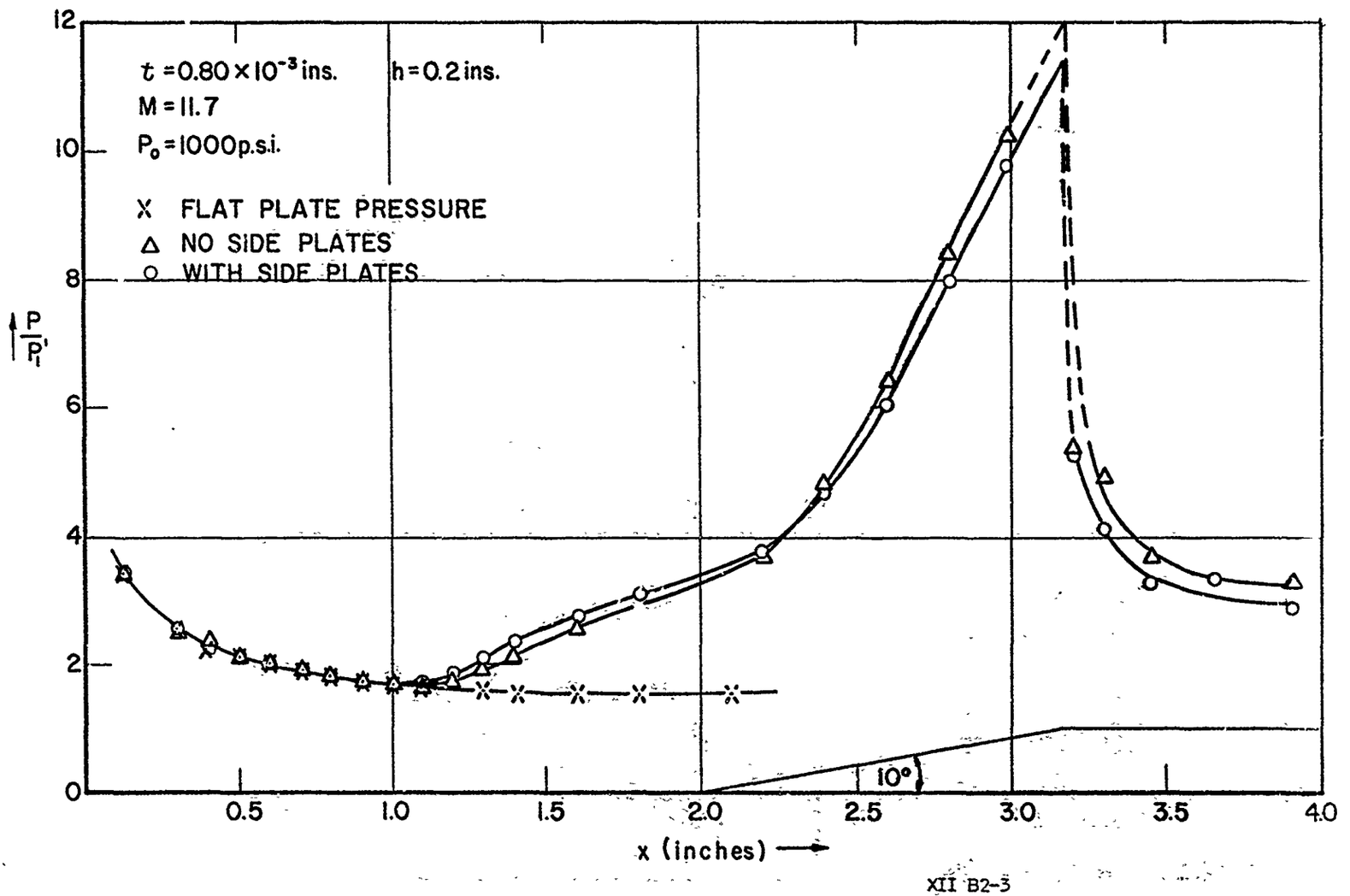

XII B2-3

Figure 9. Pressure distribution on a flat plate with a 10° wedge, with and without side plates

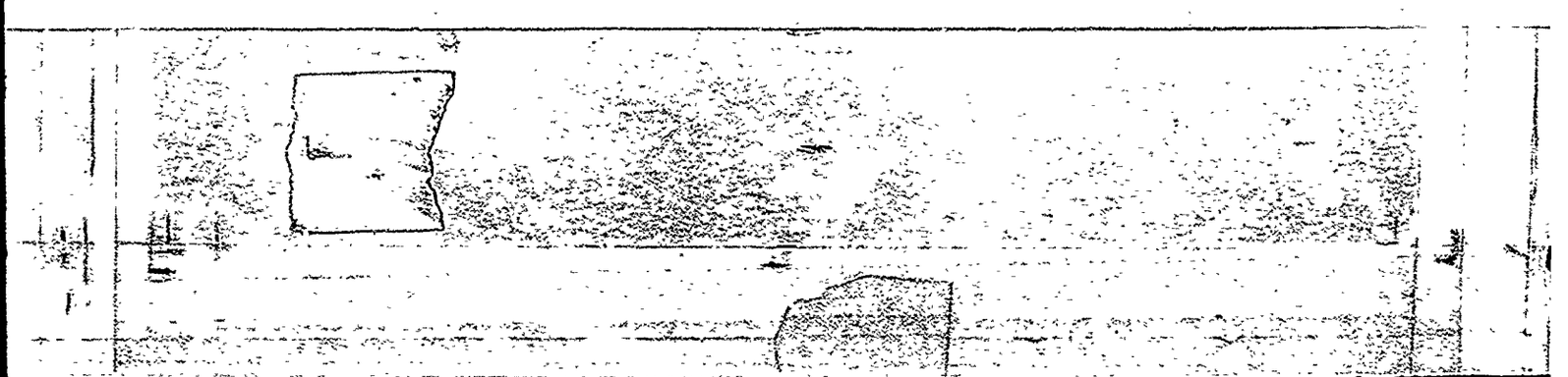

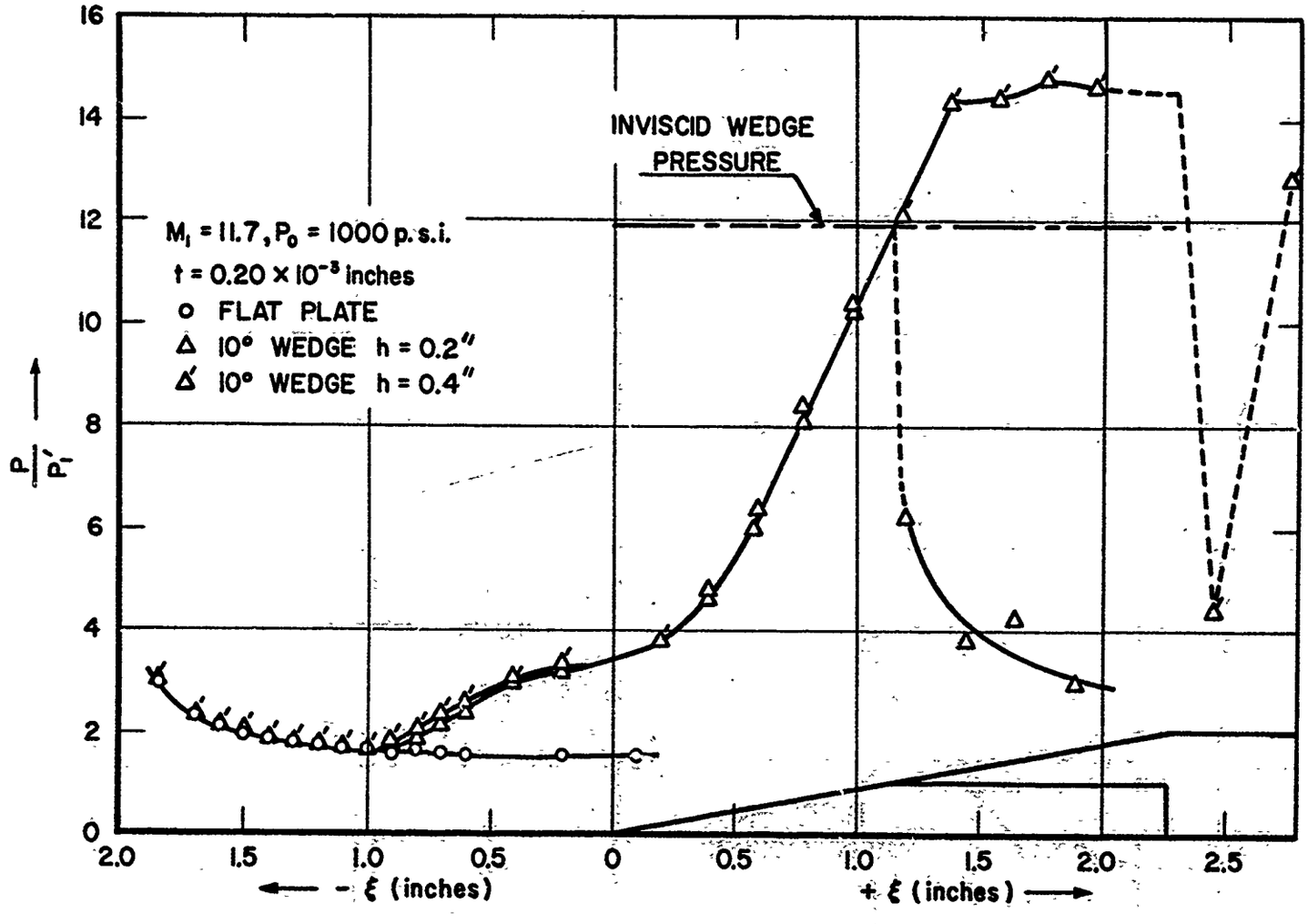

XII B2-4

Figure 10a. Pressure distribution on a flat plate with 10° wedge at M = 11.7, t = 0.20x10^{-3} inches

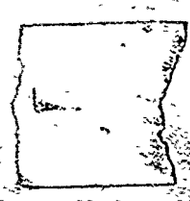

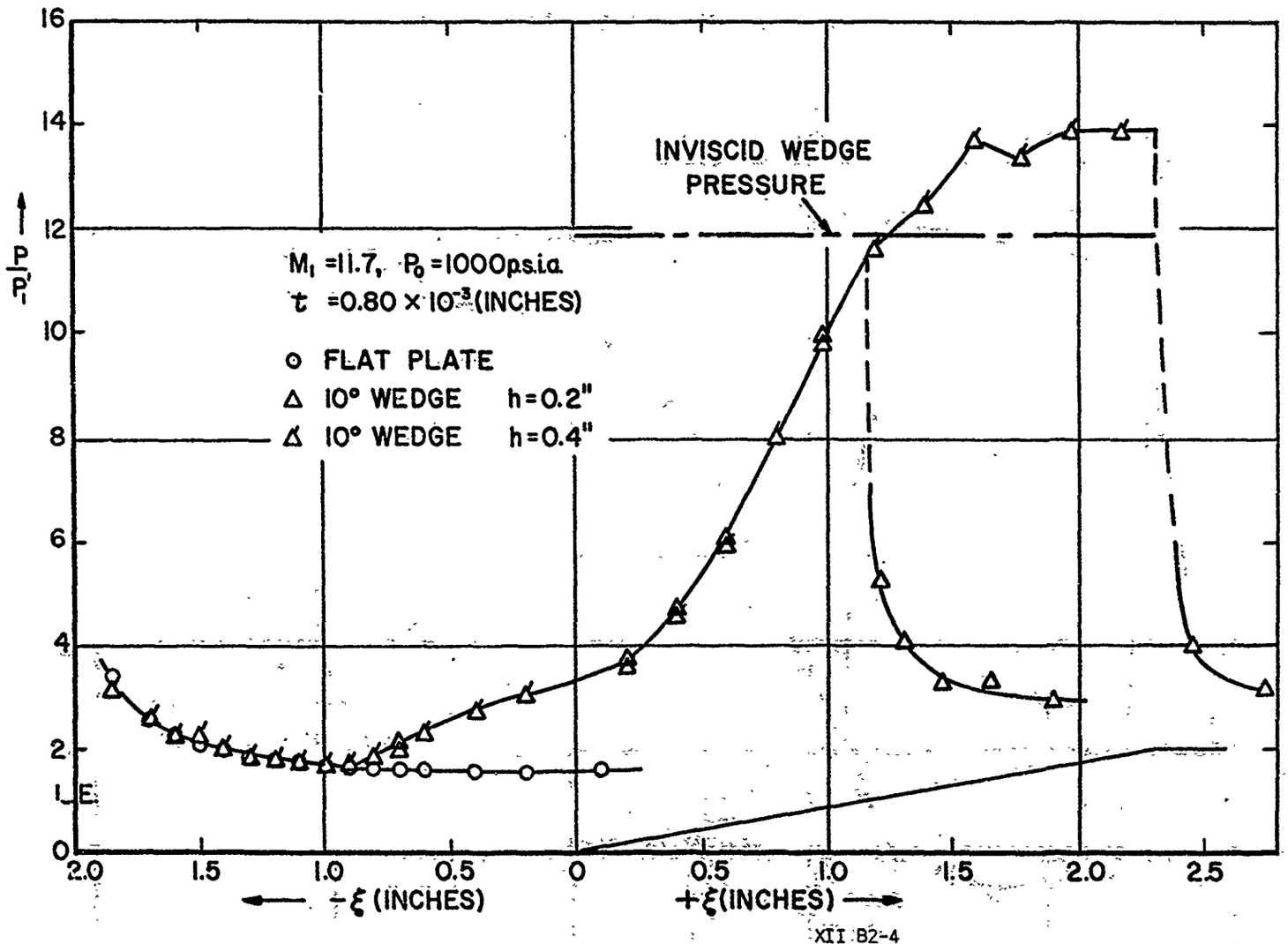

XII B2-4

Figure 10b. Pressure distribution on a flat plate with a 10° wedge at M = 11.7, t = 0.80x10^{-3} inches.

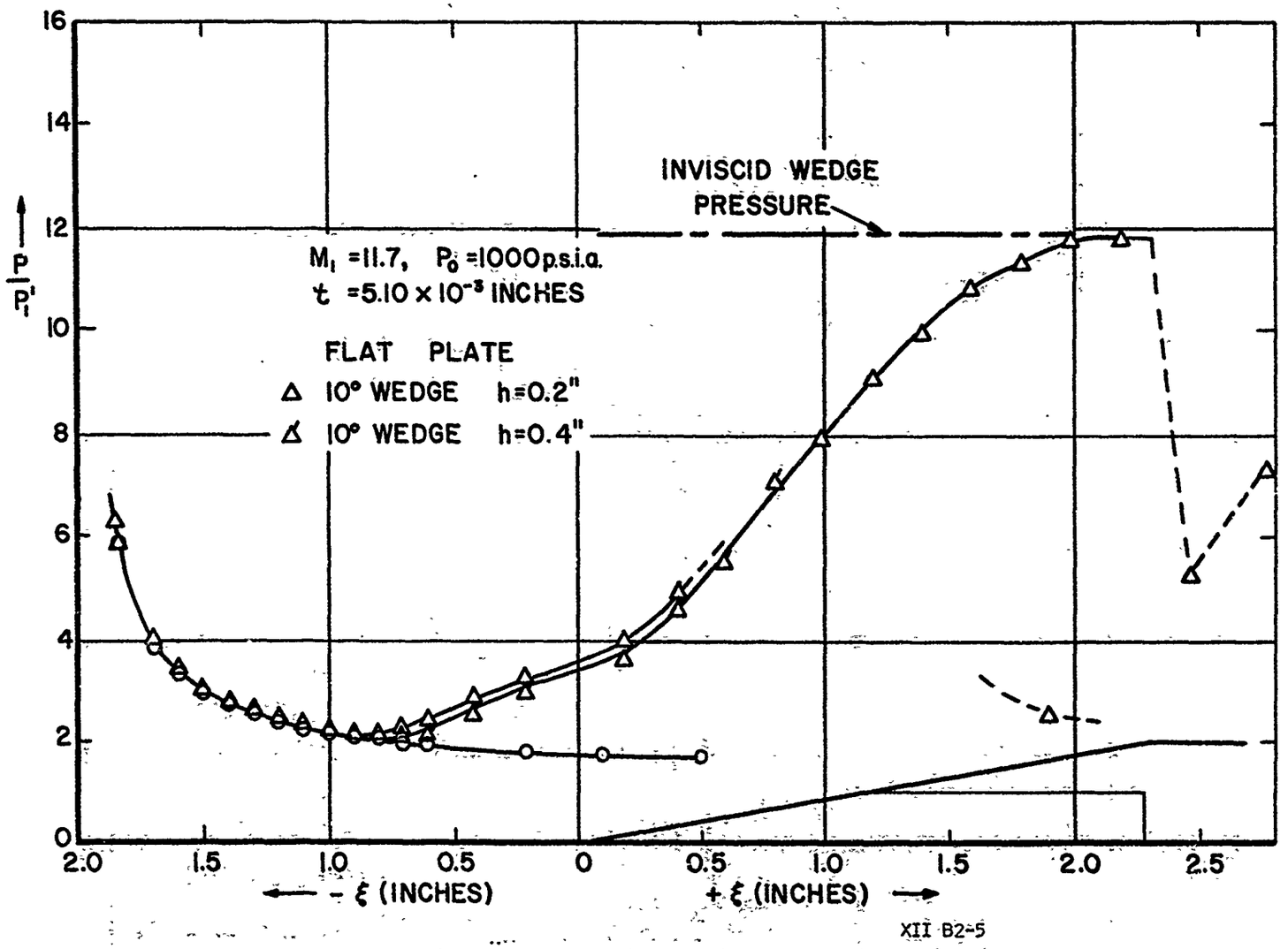

Figure 10c. Pressure distribution on a flat plate with a 10° wedge at M = 11.7, t = 5.1x10^{-3} inches

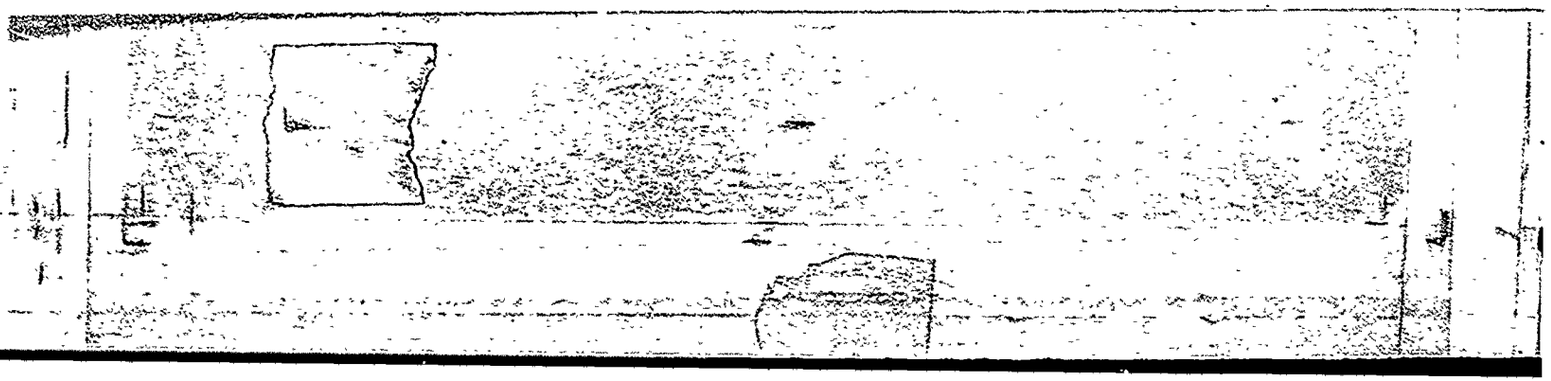

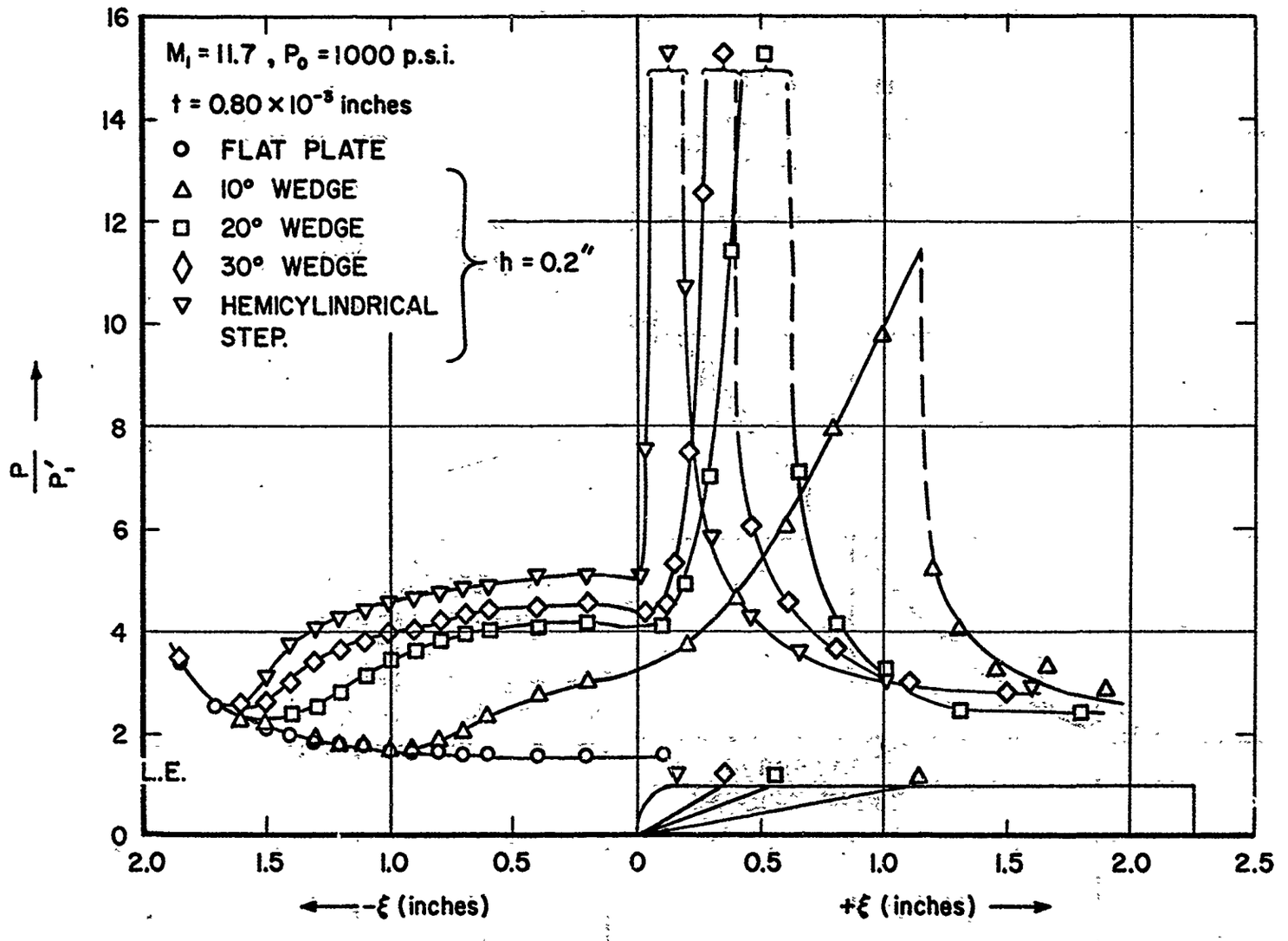

XII B2-6

Figure 11a. Pressure distribution on a flat plate and afterbody at M = 11.7, t = 0.80x10-3 inches

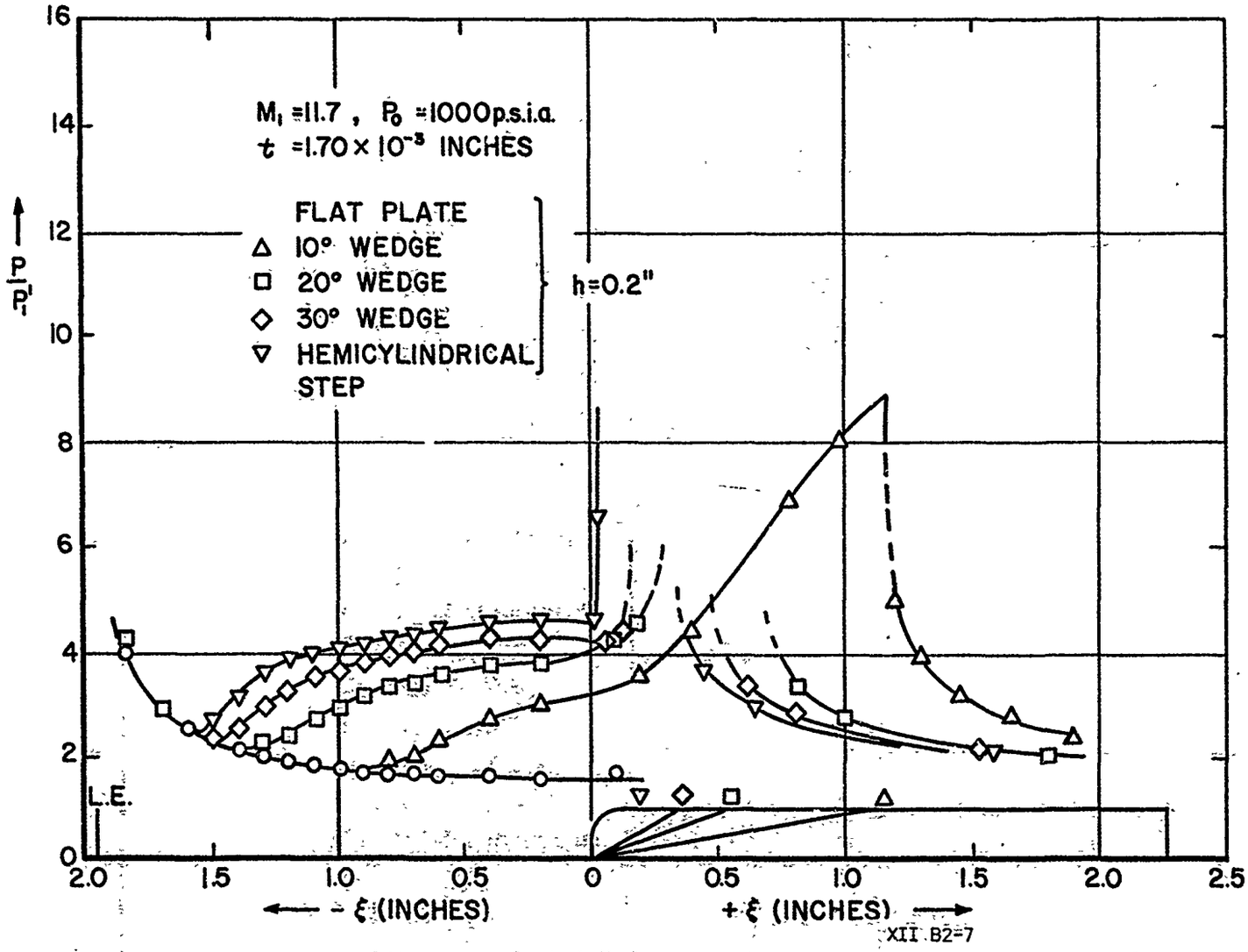

Figure 11b. Pressure distribution on a flat plate and afterbody at M = 11.7; t = 1.7x10⁻³ inches.

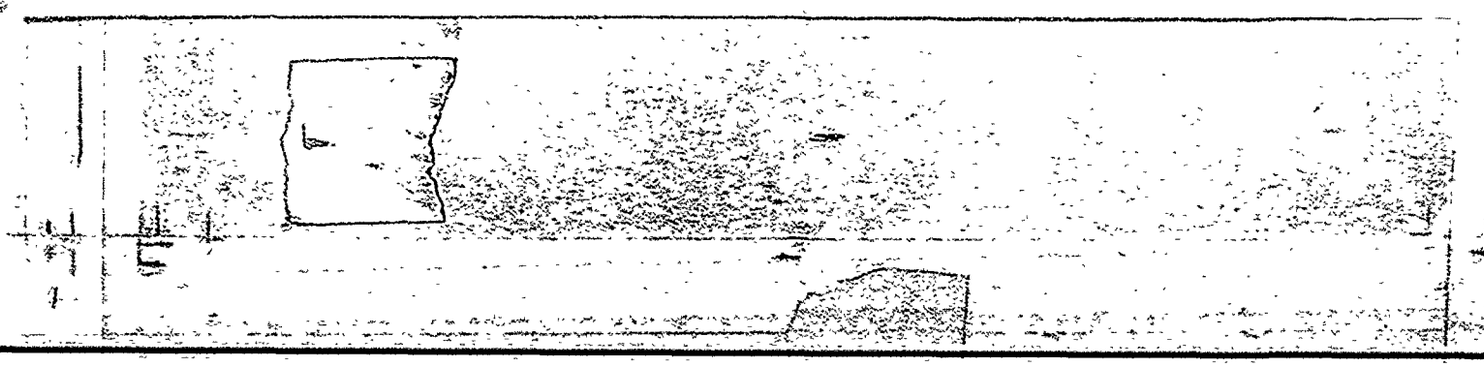

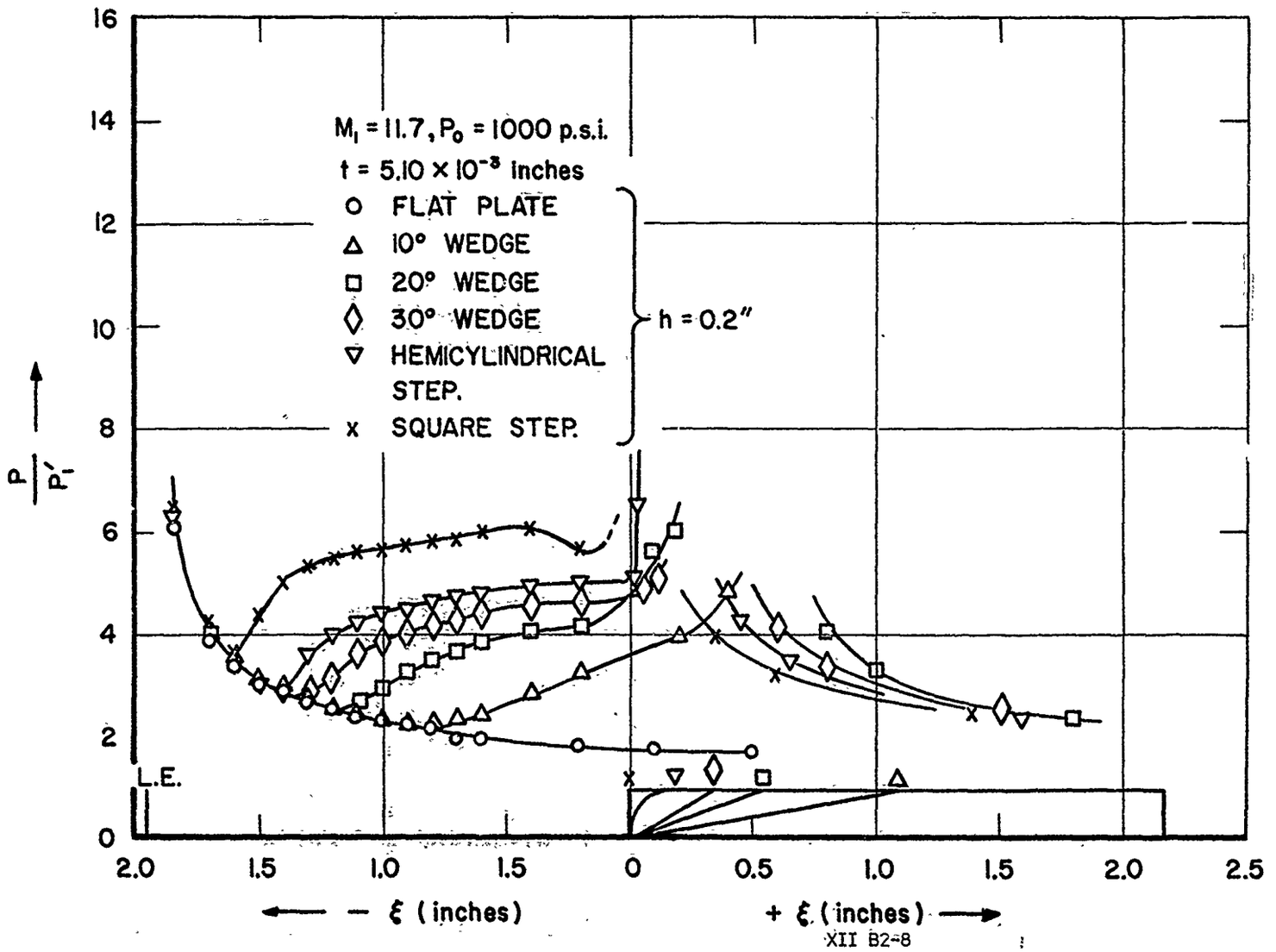

XII B2-8

Figure IIc. Pressure distribution on a flat plate and afterbody at M = 11.7, t = 5.1×10^{-3} inches

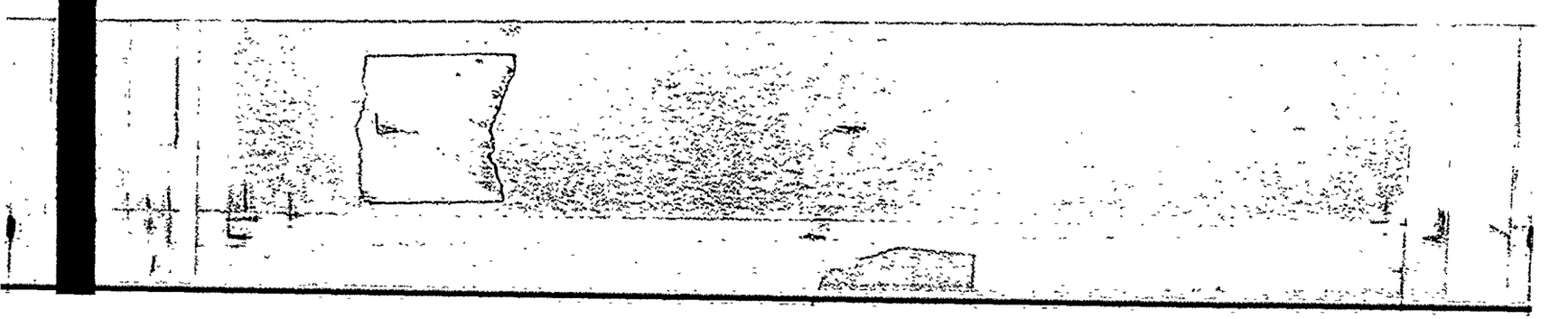

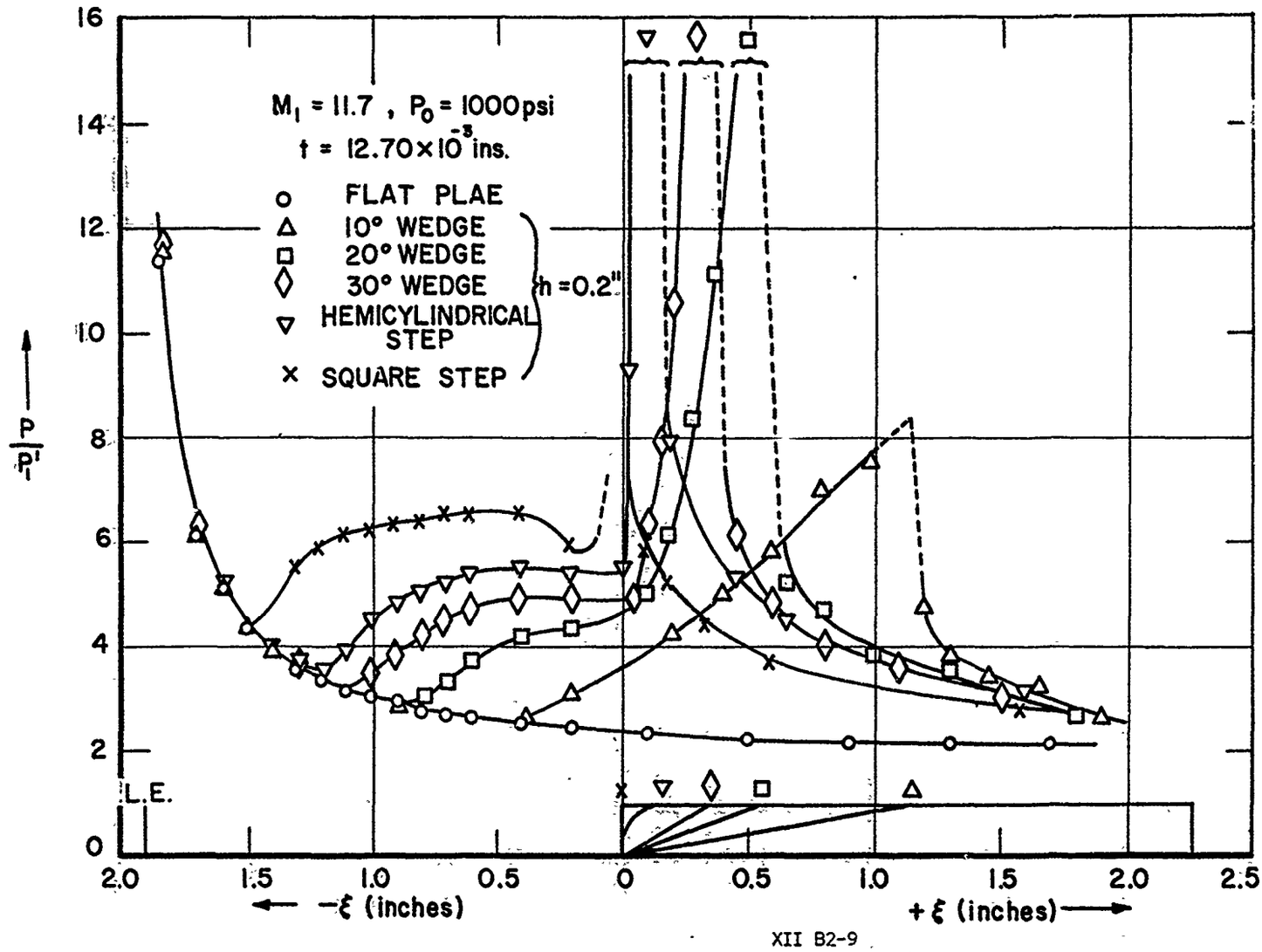

Figure IId. Pressure distribution on a flat plate and afterbody at $M_1 = 11.7$, $t = 12.7 \times 10^{-3}$ inches

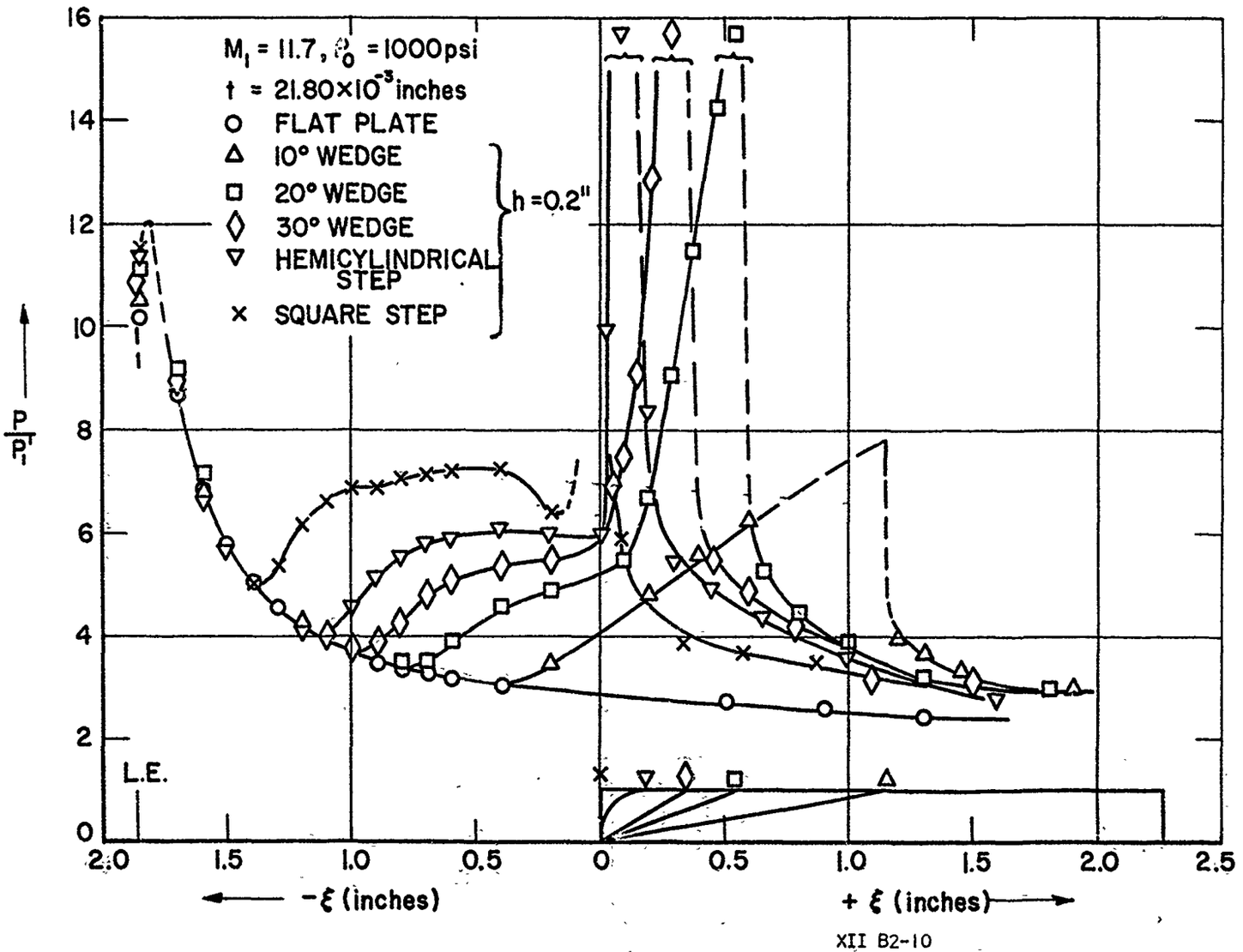

XII B2-10

Figure 11e. Pressure distribution on a flat plate and afterbody at $M_1 = 11.7$, $t = 21.8 \times 10^{-3}$ inches

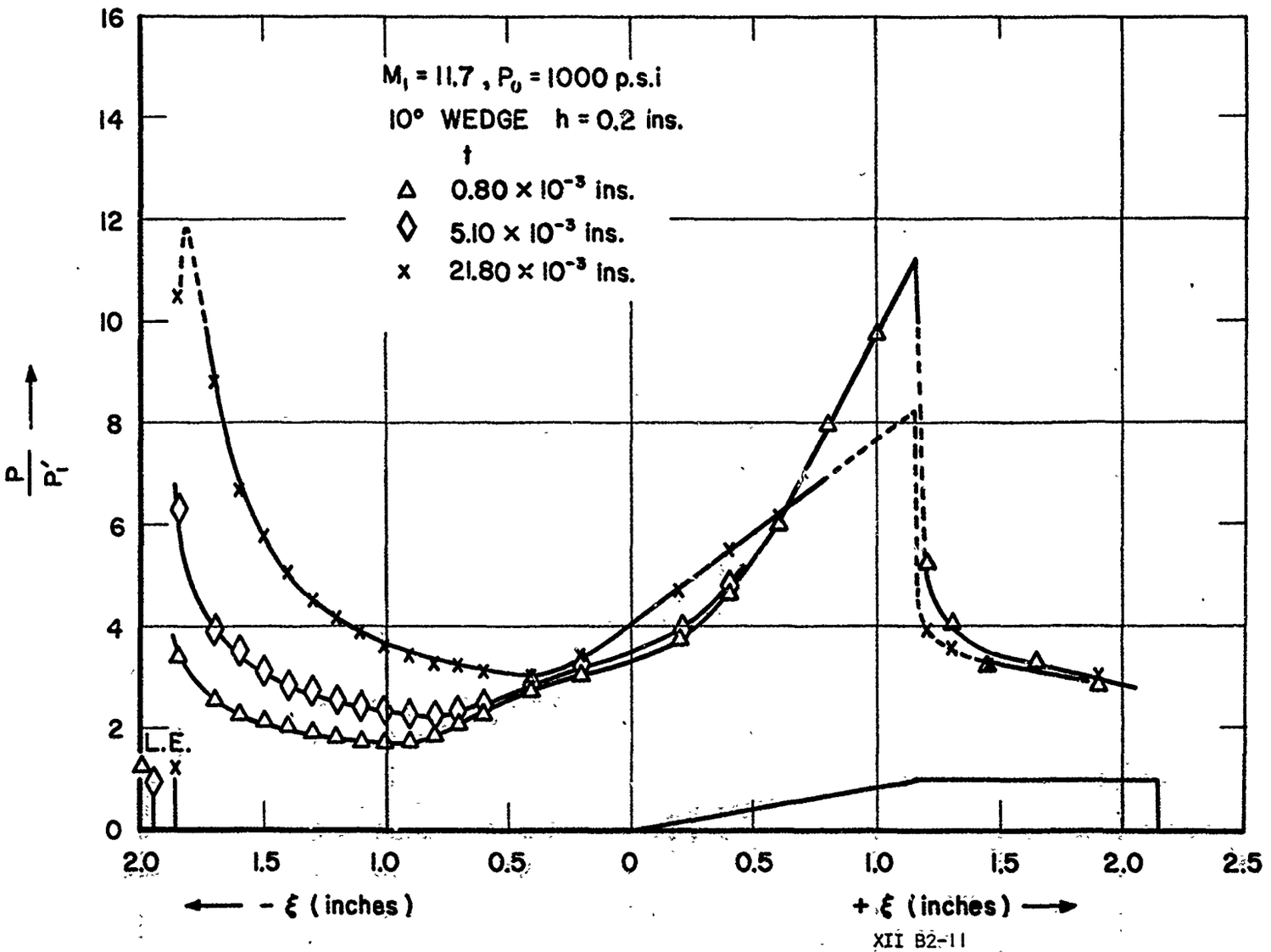

XII B2-11

Figure 12a. Pressure distribution on a flat plate and afterbody at $M_1 = 11.7$, 10° wedge

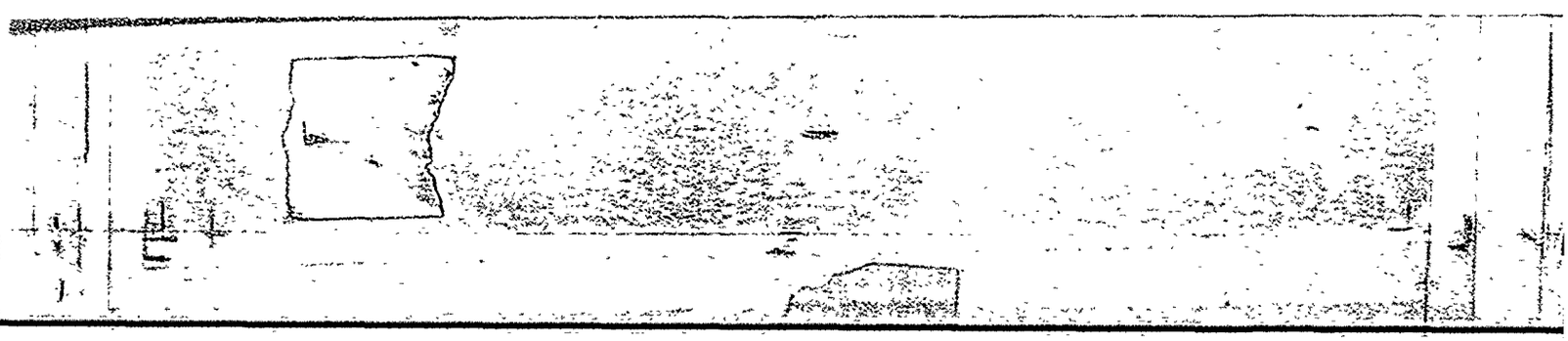

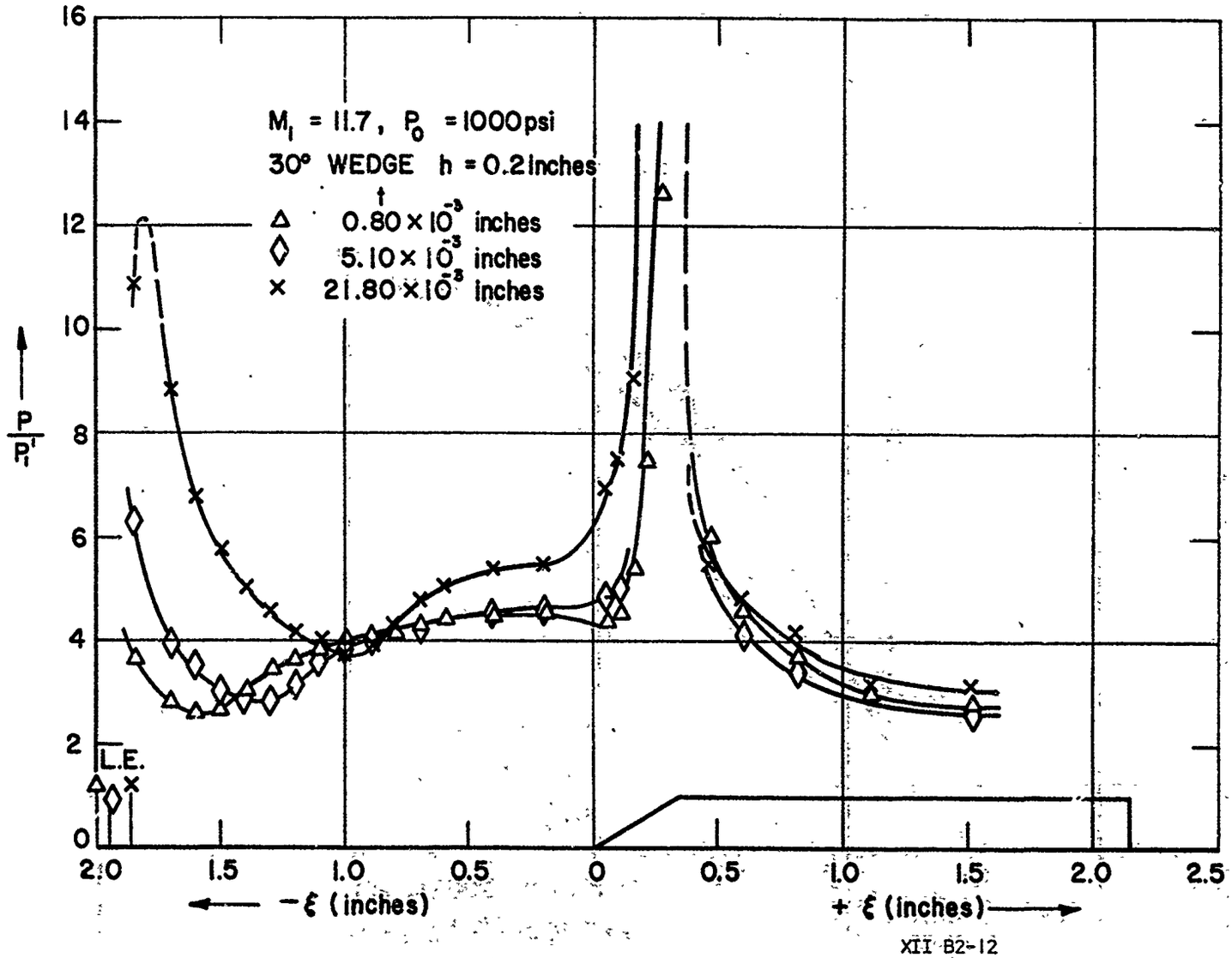

XII B2-12

Figure 12b. Pressure distribution on a flat plate and afterbody at M_1 = 11.7, 30° wedge

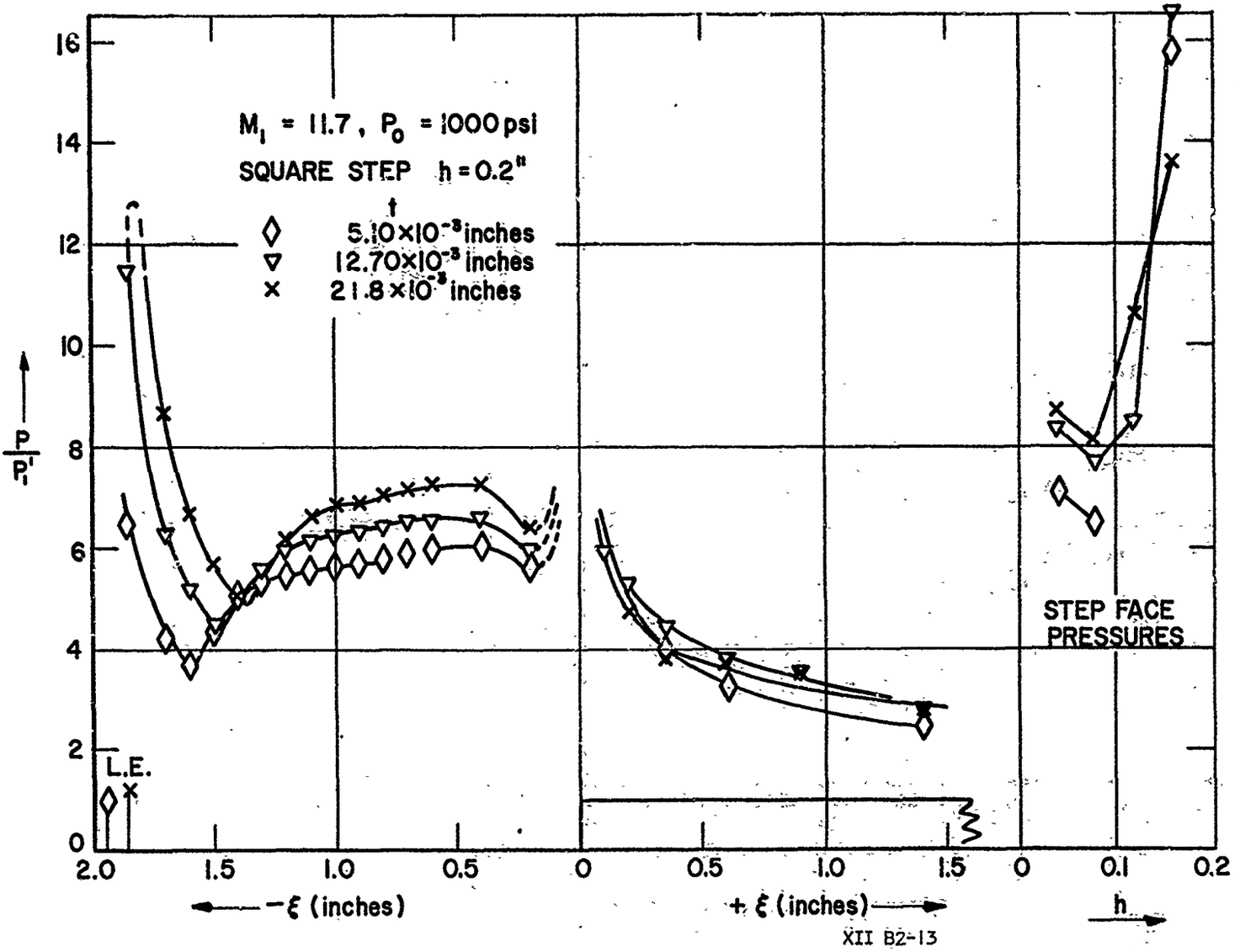

Figure 12c. Pressure distribution on a flat plate and afterbody at M_1 = 11.7, square step

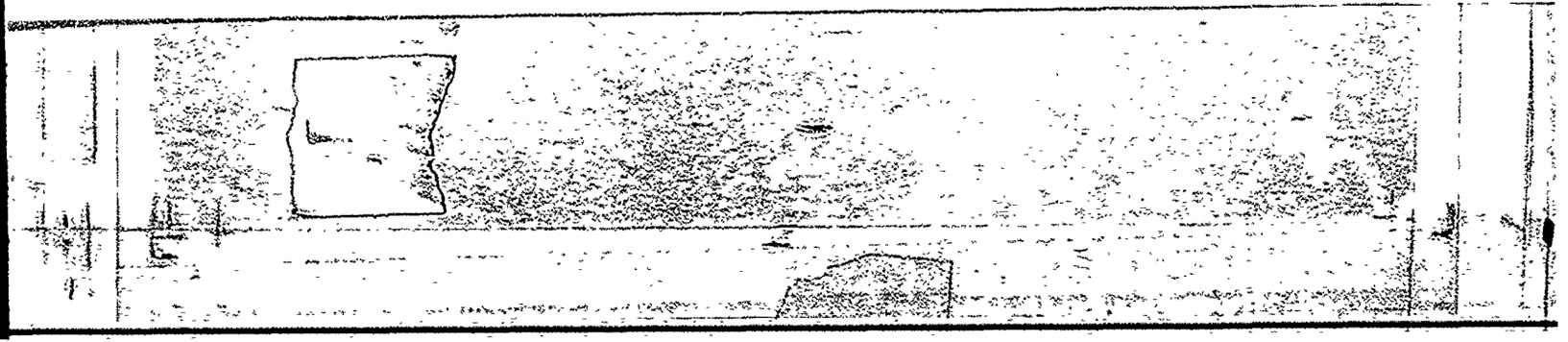

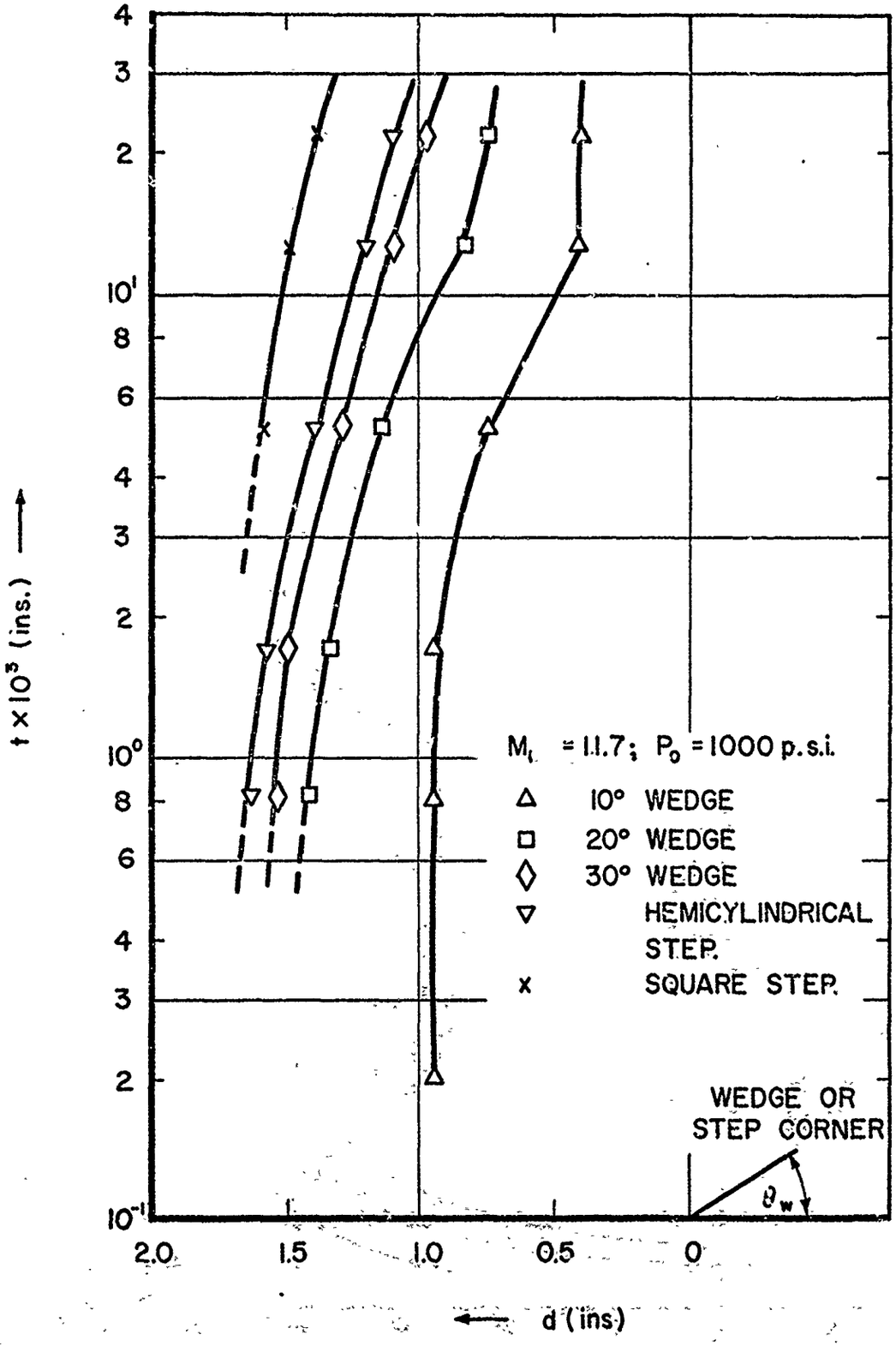

Figure 13. Variation of forward propagation of separation pressure rise with leading edge thickness for various afterbodies

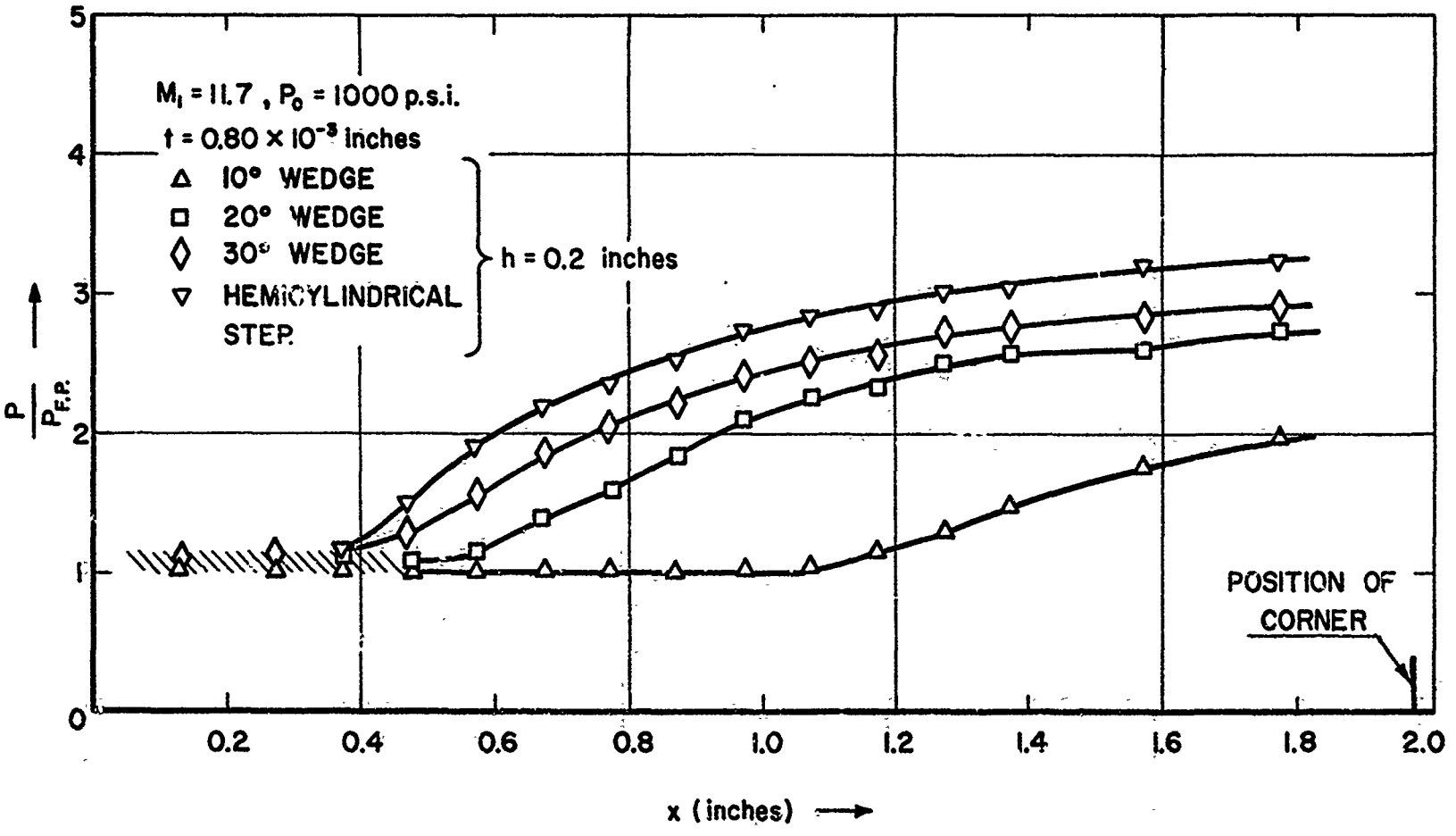

XII B2-15

Figure 14a. Pressure distribution in the separation region non-dimensionalized by the unseparated flat plate pressures, $t = 0.8 \times 10^{-3}$ inches

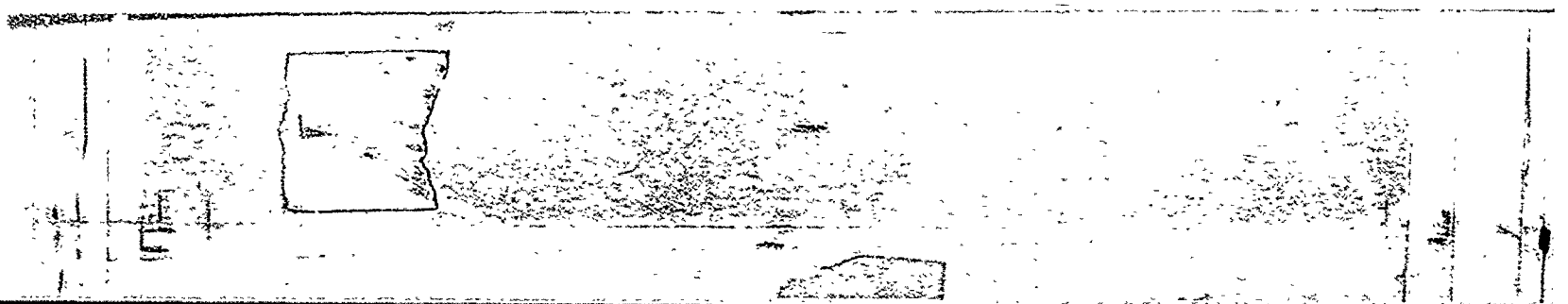

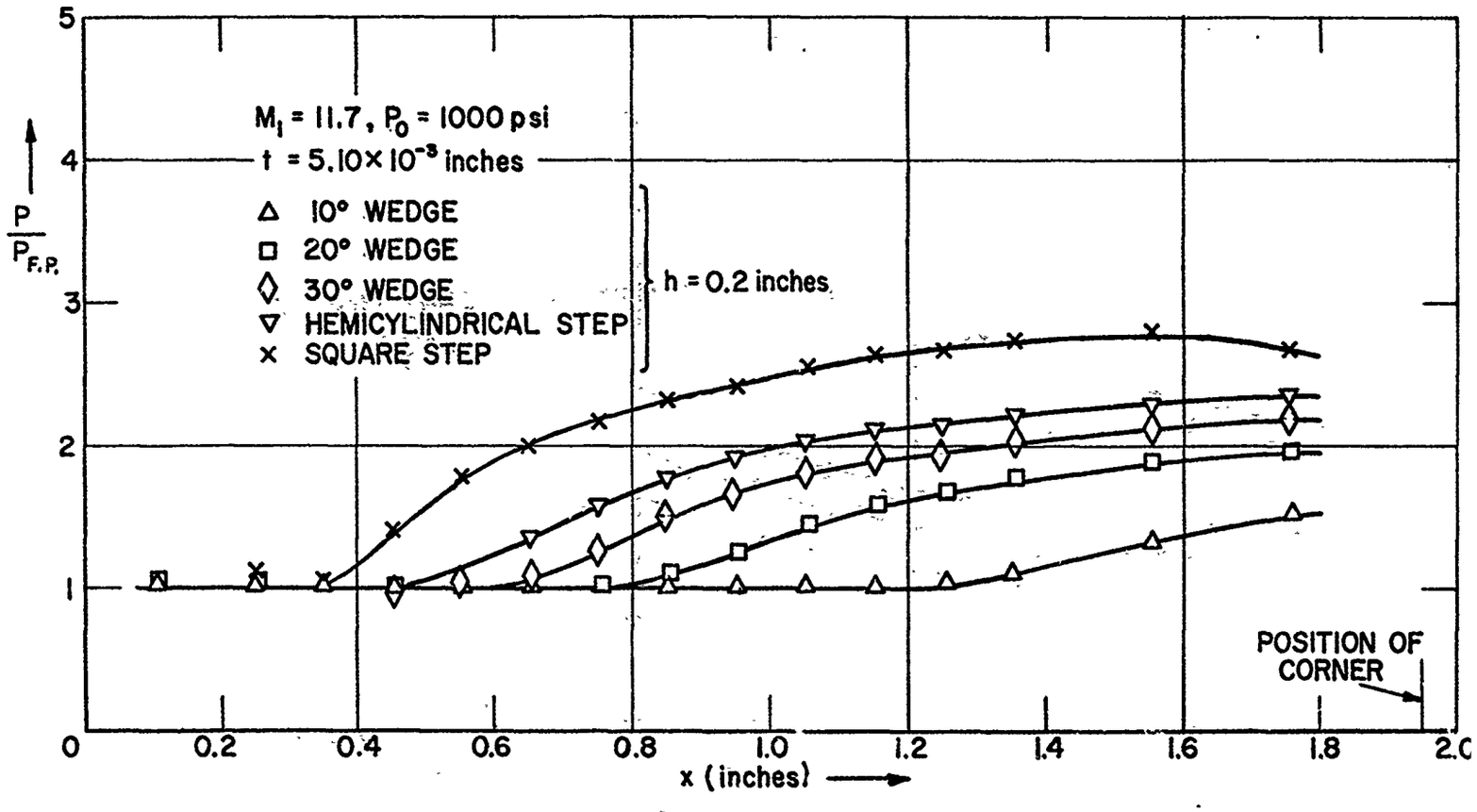

XII B2-16

Figure 14b. Pressure distribution in the separation region non-dimensionalized by the unseparated flat plate pressures, $t = 5.1 \times 10^{-3}$ inches

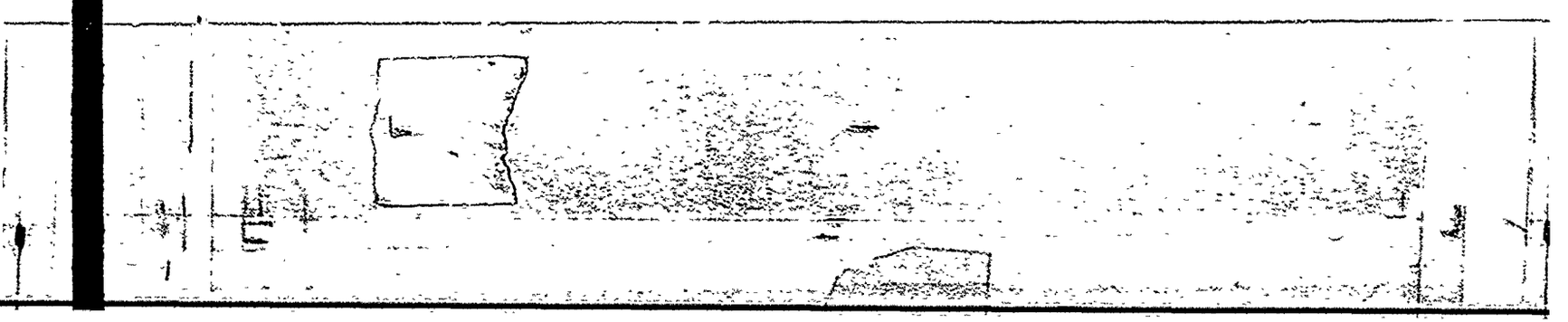

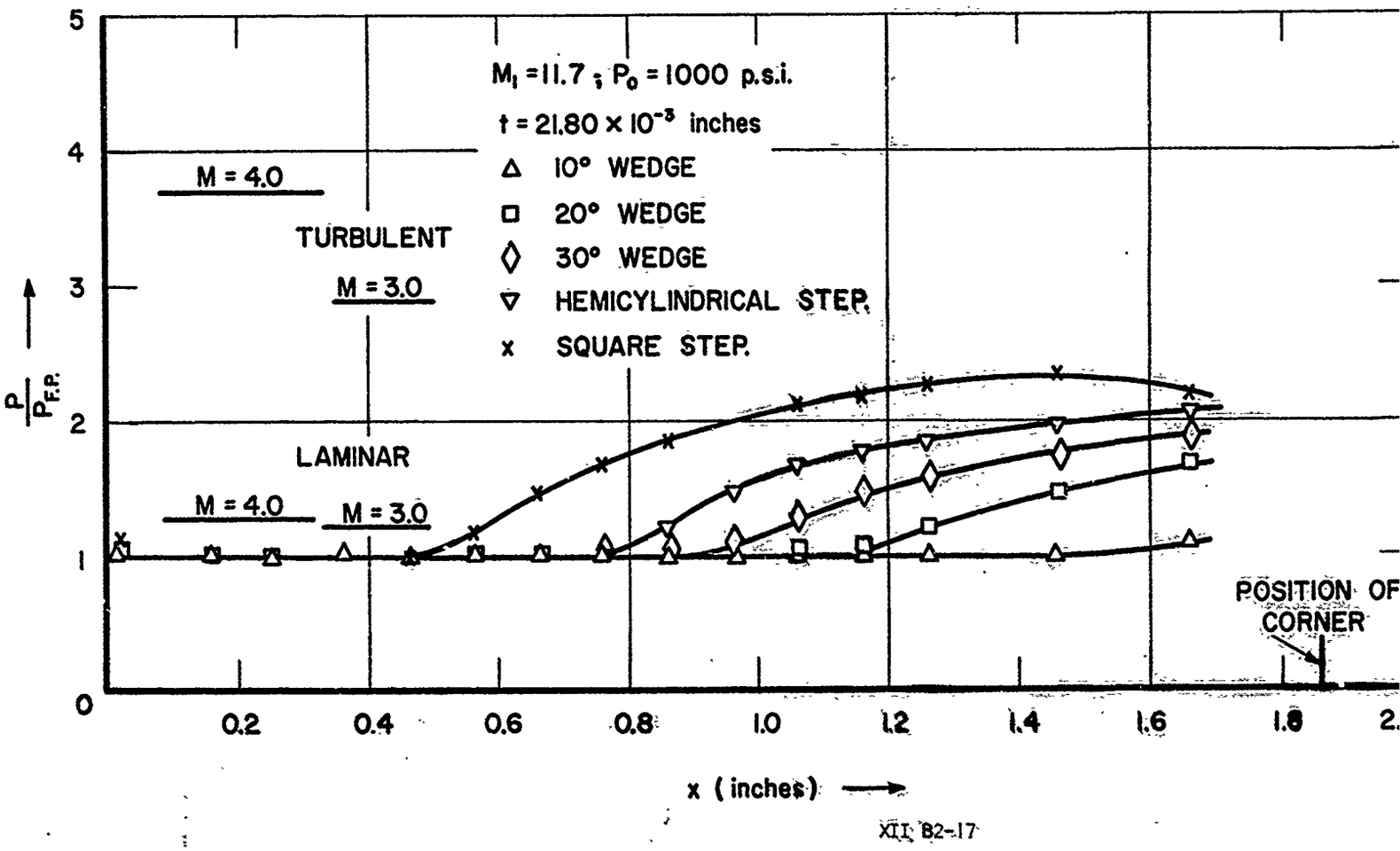

XII, 82-17

Figure 14c. Pressure distribution in the separation region non-dimensionalized by the unseparated flat plate pressures, $t = 21.8 \times 10^{-3}$ inches

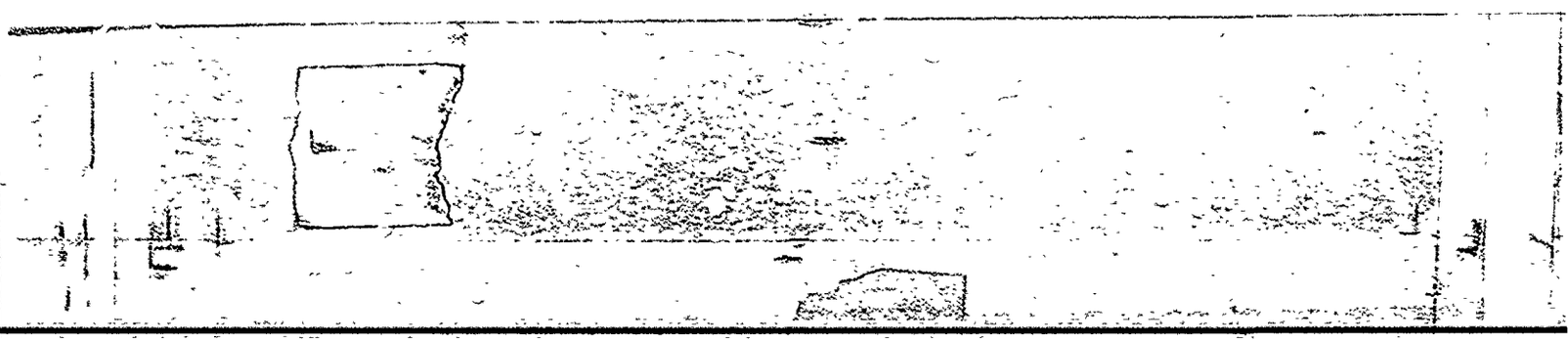

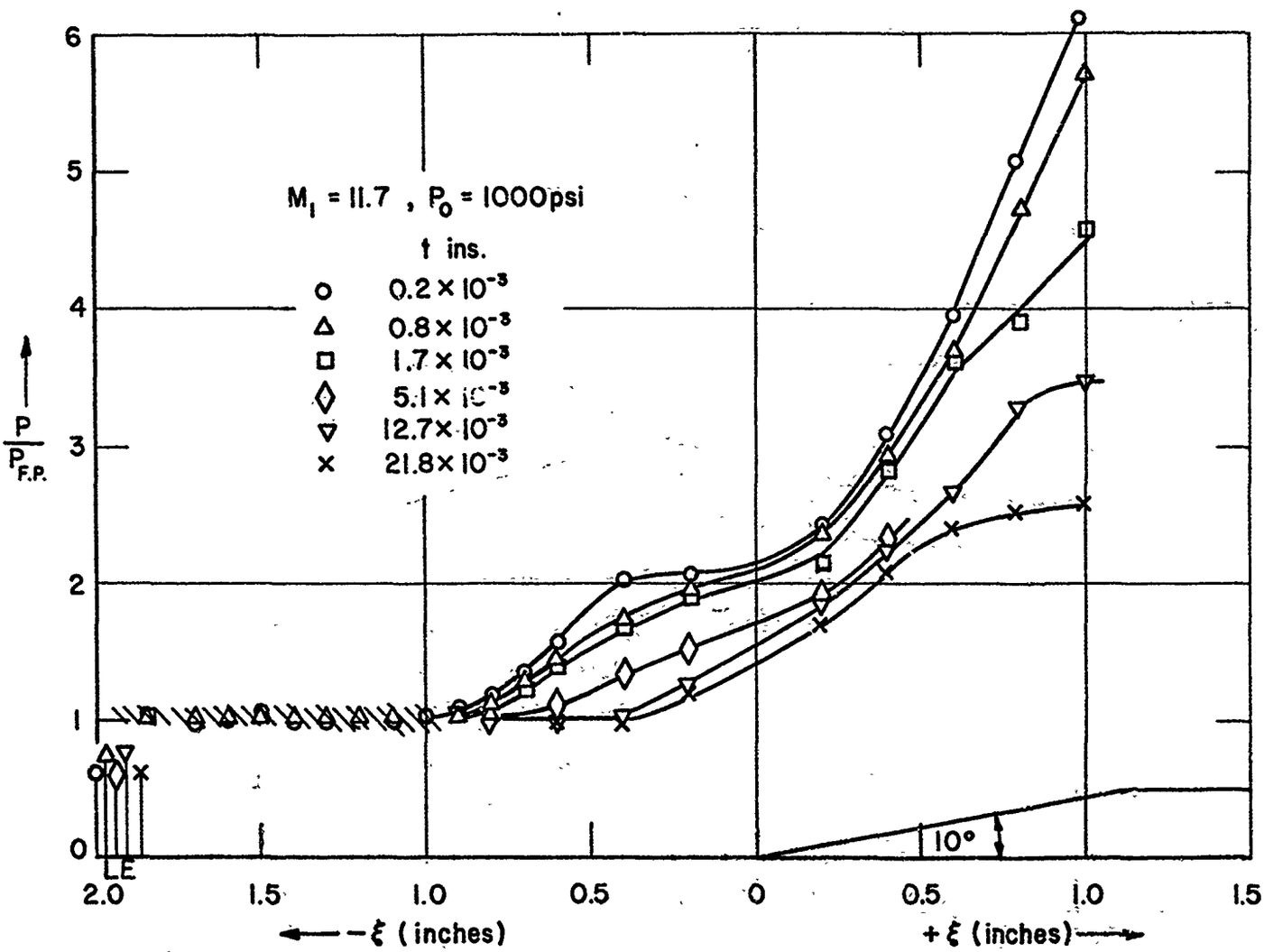

XII B2-18

Figure 15a. Pressure distribution in the separated region non-dimensionalized by unseparated flat plate pressures, 10^0 wedge

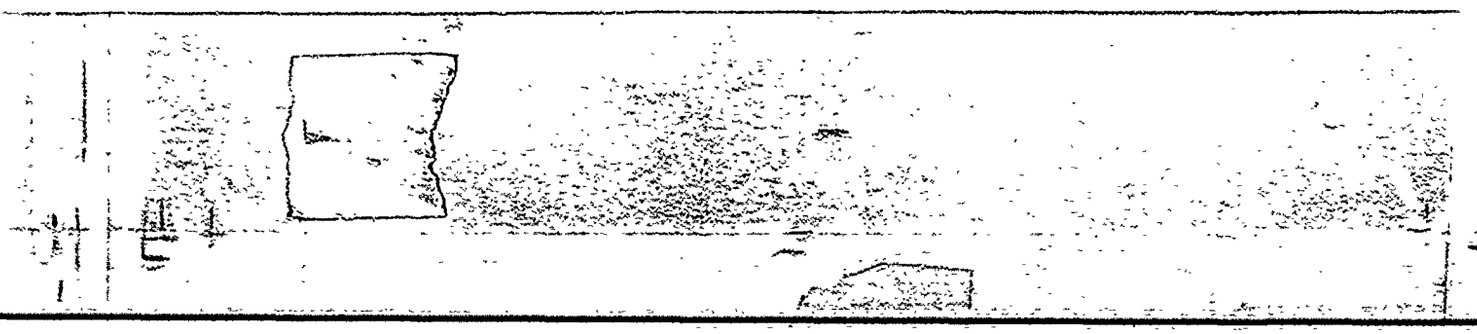

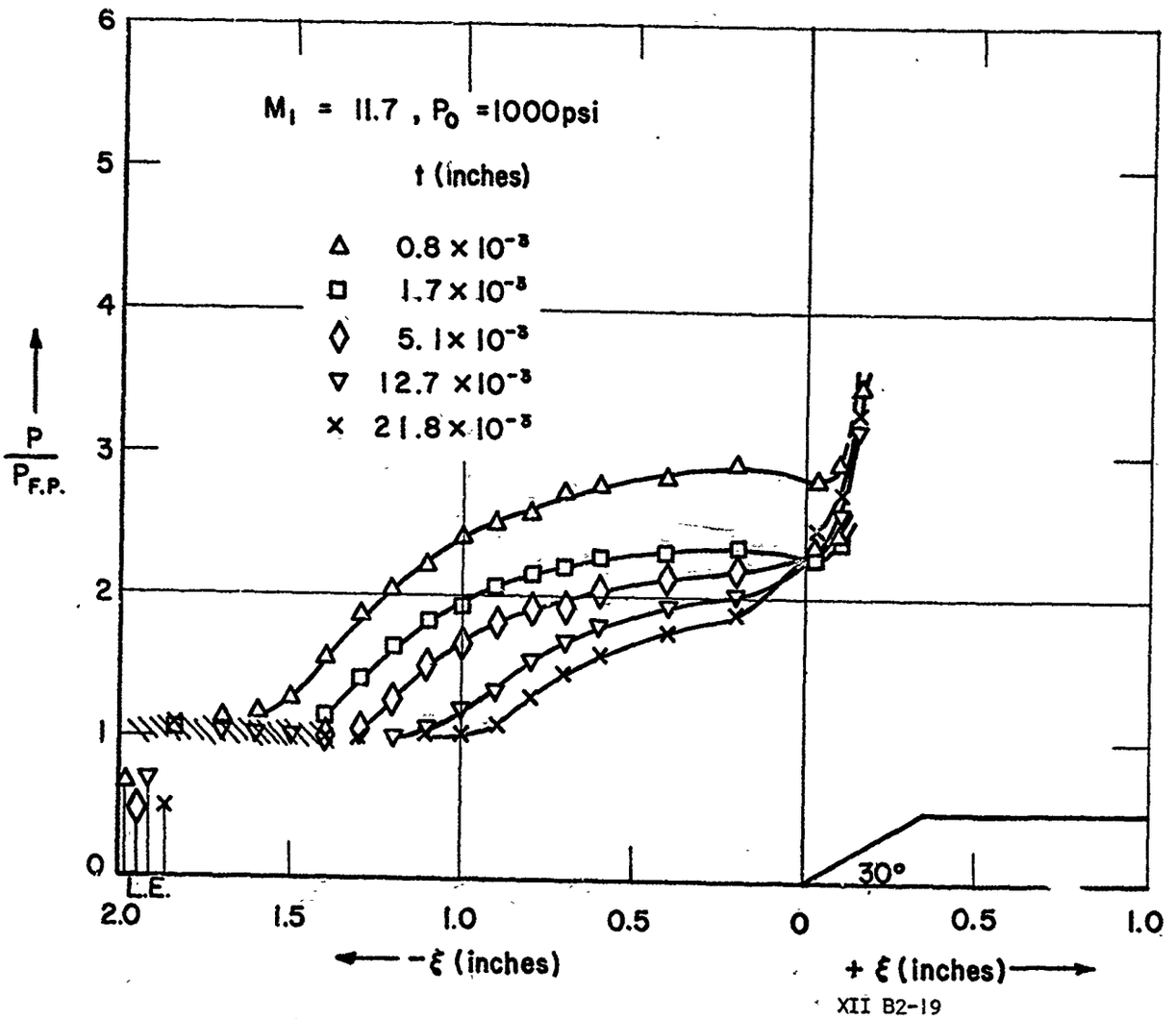

Figure 15b. Pressure distribution in the separated region non-dimensionalized by unseparated flat plate pressures, 30° wedge

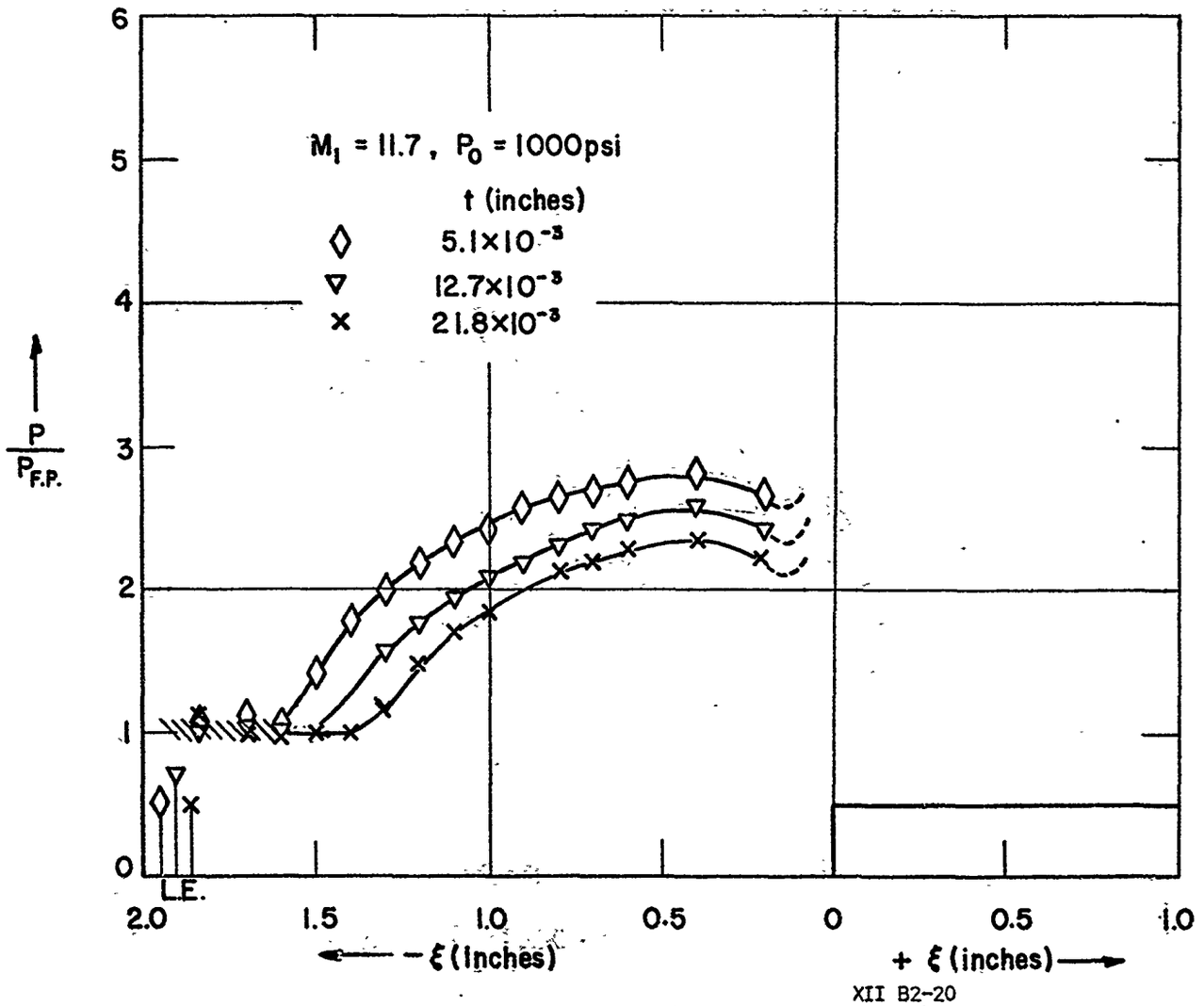

XII B2-20

Figure 15c. Pressure distribution in the separated region non-dimensionalized by unseparated flat plate pressures, square step